Title
APPLICATION OF ESCA TO THE ANALYSIS OF ATMOSPHERIC PARTICULATES

Author
Novakov, T.

Publication Date
1976-10-01

To be published as a Chapter in "Contemporary Topics in Analytical and Clinical Chemistry," Dr. David Hercules, Dr. Gary Hieftje, Dr. Merrill Evenson, and Dr. Lloyd Snyder, eds., Plenum Press

LBL-5278
c.1

APPLICATION OF ESCA TO THE ANALYSIS OF ATMOSPHERIC PARTICULATES

T. Novakov, S. G. Chang, and R. L. Dod

October 1976

Prepared for the U. S. Energy Research and Development Administration under Contract W-7405-ENG-48

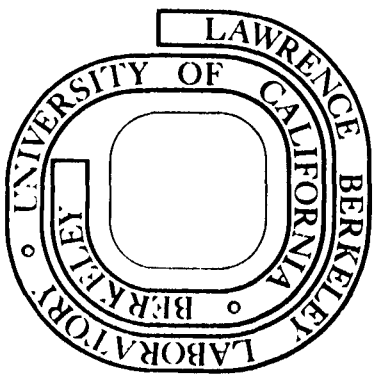

LBL-5278
c.1

DISCLAIMER

APPLICATION OF ESCA TO THE ANALYSIS OF ATMOSPHERIC PARTICULATES*

T. Novakov, S. G. Chang, and R. L. Dod

Energy and Environment Division
Lawrence Berkeley Laboratory
University of California
Berkeley, CA 94720

October 1976

ABSTRACT

This chapter reviews the application of X-ray photoelectron spectroscopy (ESCA) to the chemical characterization of ambient and source-enriched particulate matter. These analyses involve measurements of the chemical shift, core electron level splitting, relative concentrations, and volatility (in vacuum) of different particulate species. Results of the ESCA analyses are compared with results obtained by methods that determine bulk constituents. For completeness, the use of ESCA as a researh tool in aerosol chemistry is described.

---

*This work was done with support from the U.S. Energy Research and Development Administration and the National Science Foundation--RANN.

CONTENTS

1.1. INTRODUCTION

Aerosol particles (also referred to as particulate matter or particulates) play a major role in the overall air pollution problem. They are responsible for reduction of visibility and acidification of waters, and in certain size ranges are deposited in the lungs where they can cause a variety of health effects. The air pollution aerosol particles can consist of solid and/or liquid substances. Some of these, such as windblown dust, soot, and fly ash, originate in sources outside the atmosphere and are known as "primary" particles. Others are formed directly in the atmosphere by reactions among the primary particulate and gaseous species and are known as "secondary" pollutants. The nature of both these primary and secondary particulate species, as well as the extent to which atmospheric chemistry is governed by (photochemical) gas phase or heterogeneous gas-particle reaction mechanisms, is presently a very active area of research.

In order to devise an effective control strategy, the chemical species responsible for the adverse environmental and health effects must be selectively identified and the process by which these species are formed in the source effluents or in the atmosphere must be ascertained. The key to the successful accomplishment of this important task is the determination of the exact chemical composition of the compounds and species associated with these particles. It is important to determine the chemical composition of particle constituents as they actually exist in aerosol form and not, for example, as they may appear in solutions. What is required is a truly "in situ" method for chemical analysis, where the analysis would be performed without the need for collecting the particles on filters or other collection media. Reliable methods of this kind are unavailable now, however.

One must further distinguish the bulk from the surface composition of aerosol particles. Some particles or some of their major bulk constituents may eventually be soluble in body fluids, so that practically their entire content can be toxicologically harmful. On the other hand, particle surfaces may be chemically dissimilar to the interiors of the particles and may carry microscopic layers of contaminants that make contact with lung membranes, leading to exposures that have little to do with the bulk composition of the particles. An intermediate situation may exist when harmful contaminants cover the surface of extremely small particles (of the order of 100 Å or less) which coagulate into larger clusters in the atmosphere. In this case the surface composition may be undistinguishable from the bulk composition of such composite particles.

Obviously, no single method can provide satisfactory answers to all of the above problems. Wet chemical and other microanalytical procedures have to be complemented by nondestructive physical methods. X-ray photoelectron spectroscopy, also known as ESCA--Electron Spectroscopy for Chemical Analysis,[1] whose application to chemical characterization of pollution particles is described in this chapter, is one such method. For example, application of this method has helped to uncover the presence of significant concentrations of reduced nitrogen species other than ammonium in ambient aerosol particles.[2] This group of species contains, among others, certain amines and amides[3] which are not soluble in water or such solvents as benzene and therefore could not be detected by wet chemical methods. Most analyses of pollution aerosol particles have employed wet chemical methods; and on the basis of this kind of measurement,

different workers have concluded that the principal particulate nitrogen species are ammonium and nitrate ions[4] and have suggested that the most likely combination of these is ammonium nitrate and ammonium sulfate.[5] The species uncovered with the aid of electron spectroscopy have thus escaped observation by means of wet chemistry.

In this chapter we will describe the use of X-ray photoelectron spectroscopy for chemical characterization of ambient and source-enriched aerosol particles. These analyses involve measurement of the chemical shift, core electron level splitting, relative concentrations, and volatility (in vacuum) of different particulate species. Because the method of photoelectron spectroscopy has been described in great detail in a number of papers and monographs, only the fundamentals of the technique relevant to this topic will be reviewed here. Because most of the mass of airborne pollution particles consists of compounds of carbon, nitrogen, and sulfur, special emphasis will be placed on characterization of C, N, and S species. Attempts to chemically characterize some trace metals such as lead and manganese, both originating in fuel additives, will also be described.

1.2. METHOD

X-ray photoelectron spectroscopy is the study of the kinetic energy distribution of photoelectrons expelled from a sample irradiated with monoenergetic X-rays. The kinetic energy of a photoelectron E_{kin}, expelled from a subshell i, is given by $E_{kin} = h\nu - E_i$, where $h\nu$ is the X-ray photon energy and E_i is the binding energy of an electron in that subshell. If the photon energy is known, experimental determination of the photoelectron

kinetic energy provides a direct measurement of the electron binding energy.

The electron binding energies are characteristic for each element. The intensity of photoelectrons, originating from a subshell of an element, is related to the concentration of atoms of that element in the active sample volume. In principle, this feature enables the method to be used for quantitative elemental analysis. The binding energies, however, are not absolutely constant but are modified by the valence electron distribution, so that the binding energy of an electron subshell in a given atom varies when this atom is in different chemical environments. These differences in electron binding energies are known as the chemical shift. The origin of the chemical shift can be understood in terms of the shielding of the core electrons by the electrons in the valence shell. A change in the charge of the valence shell results in a change of the shielding which affects the core electron binding energies. For example, if an atom is oxidized, it donates its valence electrons and thus becomes more positively charged than the neutral configuration. Some of the shielding contribution is removed, and in general the binding energies of the core electron subshells are increased. Conversely the binding energies will show an opposite shift for the reduced species. Therein lies the usefulness of chemical shift determinations in the analysis of samples of unknown chemical composition. In practice, the measurements of the chemical shifts are complemented by the determination of relative photoelectron intensities, from which the stoichiometric information can be inferred.

The relation $E_{kin} = h\nu - E_i$ is unambiguous for gaseous samples. In solid samples, however, the photoelectron has to overcome the potential

energy barrier at the surface of the sample. This potential energy barrier is known as the work function of the sample ϕ_{sample}. However, if the solid sample is in electrical contact with the electrically "grounded" spectrometer, the Fermi levels of the sample and of the spectrometer are equalized. On entering the spectrometer a photoelectron is accelerated by $e[\phi_{sample} - \phi_{spect}]$, and as it reaches the detector it acquires the kinetic energy $E_{kin} = h\nu - E_{i,f} - \phi_{spect}$. In the experiment, therefore, the kinetic energy is determined by the spectrometer work function ϕ_{spect} and by the binding energy referenced to the Fermi level of the spectrometer $E_{i,f}$.

In order to use photoelectron spectroscopy as an analytical tool it is important to understand how different factors influence the chemical shift, and how the observed chemical shifts relate to the chemist's intuitive conception of bonding and molecular structure. We shall briefly describe some of the theoretical results on chemical shifts, insofar as they pertain to the subject of analytical applications of photoelectron spectroscopy.

The electron binding energy is defined as the difference between the total energies of the final and the initial states. An exact calculation of the total energy of even the simplest multielectron systems is impractical. Self-consistent field methods which yield rather accurate total energies are used instead. In this type of calculation the total energy of the initial state--when each core orbital is doubly occupied--is calculated first. The total energy of the final state is calculated in accordance with Koopmans' theorem,[6] i.e., assuming the same wave functions as those used for the initial state calculation except one of the orbitals is now

singly occupied. This approach assumes that the photoelectron is suddenly removed, leaving the passive orbitals "frozen." Physical justification for this approach relates to the fact that the time required for the photoelectron to leave the atom is much shorter than the lifetime of the core level hole.

The electrons in the outer shells, however, can respond quickly to the formation of the positive core hole by "shrinking" their orbitals adiabatically. This relaxation process is fast because it involves no change in the quantum state. The additional Coulomb repulsion of the shrunken orbitals causes the calculated photoelectron kinetic energy to be greater than the one obtained under the frozen orbital approximation. In other words, the effect of the relaxation is to reduce the calculated binding energy with respect to the one calculated under the assumption of strict validity of Koopmans' theorem. To take the relaxation effects into consideration, the total energy of the final state is calculated for the core hole state instead of the ground state where all orbitals are doubly occupied. Several approaches to this problem have been investigated by Bagus,[7] Rosen and Lindgren,[8] Schwartz,[9] Brundle et al.,[10] and Siegbahn[11] among others.

Alternative theoretical approaches have been developed to calculate the binding energies from the frozen orbital model corrected for relaxation effects. Hedin and Johansen[12] formulated a correction to the binding energy obtained from Koopmans' theorem by including the polarization potential created by the presence of a hole in the core orbital. Snyder[13] considered the problem of orbital relaxation in an atom from which an inner shell electron has been ejected and discussed the hole effect in

in terms of atomic shielding constants. Lieberman,[14] and Manne and Åberg[15] have considered the relationship between hole state and frozen orbital calculations based on physical insight.

Theoretical approaches such as those listed above are valuable in elucidating the contributions of various factors to the chemical shift, but such calculations are of limited value to calculate theoretically the binding energies or binding energy shifts for molecules of practical interest.

Fortunately, however, the experimentally observed chemical shifts are well correlated with certain parameters directly related to conventional ideas about chemical structure. For example, even in the early stages of photoelectron spectroscopy it was realized that the chemical shifts can be related to the oxidation state of the atom in a molecule. Subsequently, attempts to correlate the binding energy shifts with the estimated effective atomic charges were made. Electronegativity difference methods,[16,17] the extended Hückel molecular orbital method,[18] and the CNDO method[19-21] were used to calculate the effective charge. Only rough correlations were obtained, however. It was subsequently found that the poor correlations result from neglect of the potential generated by all charges in the molecule.

Chemical shifts can be adequately described by the electrostatic potential model in which the charges are idealized as point charges on atoms in a molecule. The electron binding energy shift, relative to the neutral atom, is equal to the change in the electrostatic potential resulting from all charges in the molecule as experienced by the atomic core under consideration. Different approaches to the potential model calculations were used by Gelius et al.,[22,23] Siegbahn et al.,[17,24]

Ellison and Larcom,[20] and Davis et al.[21] Detailed theoretical analysis of the potential model were given by Basch[25] and Schwartz.[26]

In practice, line broadening and the small magnitude of the chemical shifts may make the determination of even the oxidation state difficult in some cases. Because of this difficulty in cases of transition metal compounds, the "multiplet splitting" effect can be employed to infer the oxidation state. Multiplet splitting of core electron binding energies[27] is observed in the photoelectron spectra of paramagnetic transition metal compounds. In any atomic or molecular system with unpaired valence electrons, the 3s-3d exchange interaction affects the core electrons differently, according to the orientation of their spin. This causes the 3s core level to be split into two components. For example, in an Mn^{2+} ion whose ground state configuration is $3d^5\ ^6S$, the two multiplet states will be ^7S and ^5S. In an Mn^{4+} ion having the ground state configuration $3d^3\ ^4F$, the two spectroscopic states will be ^5F and ^3F. In the first approximation, the magnitude of the multiplet splittings should be proportional to the number of unpaired 3d electrons. Hence the Mn(3s) splitting will be greatest for Mn^{2+} ions and least for Mn^{4+}.

Because of the low energy of photoelectrons induced by the most commonly used Mg or Al X-rays, the effective escape depth for electron emission without suffering inelastic scattering is small. Recent studies have given electron escape depths of 15 to 40 Å for electron kinetic energies between 1000 and 2000 eV.[28] This renders the ESCA method especially surface sensitive and thus useful in surface chemical studies. Because of the high energy resolution, the electrons which have escaped the solid sample without energy loss are well separated from the low

energy electrons whose energy has been degraded by the inelastic collisions. The chemical shift measurements are performed only on electrons with no energy loss.

1.3. ANALYTICAL ASPECTS OF ESCA

During recent years, a number of papers and reviews have discussed the qualitative and quantitative analytical aspects of ESCA. Generally, it appears that the principal sources of uncertainty and error in ESCA analytical determinations are related to: 1) electron energy loss processes, 2) electron escape depth variations, 3) binding energy calibration procedures, and 4) sample exposure to vacuum and X-rays during analysis. The first two of these problems may have major repercussions for the determination of concentrations of elements and species in chemically heterogeneous samples. The third problem influences the validity of the assignment of chemical states through the determination of chemical shifts. Finally, the spectrometer vacuum and heating of the sample by the X-ray source may be the cause of losses of volatile species. These problems are of a general nature and obviously have to be taken into account in the analysis of atmospheric particulate matter by ESCA.

In this section experimental results and conclusions on some of the problems that relate to the analytical application of ESCA will be reviewed. These results deal with different specific objectives which are felt to be equally applicable to the topics of this chapter.

Wagner[29] has determined a table of relative atomic sensitivities, which enables the conversion of photoelectron peak intensities to relative atomic concentrations of elements in a sample. Wagner's study, as well

as the one by Swingle,[30] indicates that ESCA can be used as a semi-quantitative ($\lesssim$ 50% relative error) or even as a quantitative ($\lesssim$ 10% relative error) method when comparing chemically similar samples. Unfortunately, both of the above authors found that the relative photoelectron intensities obtained with chemically dissimilar samples show wide variations. For example, Wagner's[29] data on the Na(1s)/F(1s) intensity ratios (corrected for stoichiometry) for a number of sodium and fluorine containing compounds were found to vary by as much as a factor of 2.

Swingle[30] has attributed the observed variations in the apparent sodium and fluorine atomic sensitivities to the differences in the structure of the photoelectron energy loss spectrum. In cases of chemically similar samples, however, the same mechanism should be responsible for inelastic electron scattering.

The effect of the chemical form of an atom on the relative intensity of the photoelectron peak arising from that atom has been studied in detail by Wyatt, Carver, and Hercules.[31] They have demonstrated that different lead salts show different atomic sensitivities and have suggested that the escape depth for lead salts depends on the crystalline frame surrounding the lead cation and its coordination number, because the observed differences in sensitivities could not be accounted for by inelastic electron scattering alone. These findings imply that elemental analysis must be done with great caution, unless the chemical form of the elements in the sample is well defined. Since in many "real world" systems the exact chemical form of elements is not necessarily known, the above authors suggest that all of the elements to be measured should be

converted into the same crystalline form. However, this approach, even if feasible, would of course eliminate the nondestructive nature of ESCA analysis.

It was already mentioned that quantitative analysis by ESCA is reliable when chemically similar materials are used. Furthermore, in cases of homogeneous mixtures ESCA can be used to determine bulk composition, in spite of the surface sensitivity of the method. Thus Siegbahn et al.[23] determined the percentages of copper and zinc atoms in various alloys. Larson[32] has performed a similar study on various gold-silver alloys. Swartz and Hercules[33] were able to do quantitative analysis of MoO_2-MoO_3 mixtures by measuring the chemically shifted molybdenum peaks. Obviously, in order to accurately determine the concentration ratios of the bulk constituents, the inhomogeneities throughout the effective sample volume must be of the order of the electron escape depth or less.

The bulk sensitivity of ESCA can be estimated at approximately 0.15% based on bulk percentage. Therefore ESCA is not a "trace element" technique in the usual sense. However, because of the possibility of detecting as little as 0.1% of a monolayer[34] (about 10^{12} atoms), the absolute sensitivity of ESCA is in the picogram range. Thus ESCA is a unique trace method if the analysis is confined to preferentially surface located species. A potentially very rewarding approach to the analysis of solid substances is to perform ESCA and bulk-type measurements (for example, X-ray fluorescence) on the same sample. A proper analysis of such data would enable differentiation between preferentially surface and bulk species.

The topics discussed thus far in this section pertain essentially to the determination of relative concentrations of elements and species.

The importance and uniqueness of ESCA, however, are in its capability to measure the chemical shifts which contain implicit information about the molecular forms. The principal difficulty encountered in chemical shift measurements pertains to the calibration procedure used to account for the electrostatic charging of the sample. Hercules and Carver[35] list four basic calibration approaches which have been used. These make use of 1) contamination carbon, 2) admixed species, 3) vapor deposition of noble metals, and 4) sample constituents as internal calibration standards.

Because of low concentrations and interfering lines, it may be difficult in some cases to measure the binding energy accurately. However, as pointed out by Brinen[36] in referring to the application of ESCA to catalysts, differences in binding energies between treated or untreated catalysts and differences in relative intensities are often more informative. Subtle changes in chemical bonding, resulting either in a broadened line or in the appearance of "shoulders" on the peaks of spectra from starting material, imply formation of new species which may be crucial to the understanding of catalytic activity. Problems associated with ESCA analysis of atmospheric matter and the surface chemical reactions leading to its formation are similar to the problems mentioned above.

1.4. APPLICATION OF ESCA TO PARTICULATE ANALYSIS

1.4.1. Effect of Sample Composition at Relative Intensities

Effects of the kind described above may seriously limit the applicability of ESCA for the analysis of atmospheric particulates. Therefore, it is important to assess the usefulness of 1) photoelectron peak intensities for inferring the likely stoichiometry of certain compounds, for

example, to distinguish between ammonium sulfate and ammonium bisulfate; and 2) the relative photoelectron peak intensities for determination of relative concentrations of elements and chemical species in particulate matter. We have investigated the possible effects of the chemical composition and the surrounding matrix on photoelectron peak intensities, using heterogeneous samples that reasonably simulate the situation found in ambient particulates.

The first set of these experiments investigated the constancy of the intensity ratios of S(2p) and N(1s) photoelectron peaks, corrected for stoichiometry, for a number of pure sulfur and nitrogen containing compounds. (The nitrogen and sulfur peak intensities were normalized to the number of corresponding atoms in the molecular unit.) The resulting peak intensity ratios are displayed in Figure 1, in the order of increasing molecular weight per nitrogen atom. The mean value for peak intensity ratios of these samples is 1.65 $\pm$0.21 (1σ).

The results indicate that within an uncertainty of $\pm$15% the photoelectron peak intensities of nitrogen and sulfur reflect the relative abundances of these atoms in the compounds. These results are consistent with results reported by others, considering that the compounds examined are primarily ionic compounds containing ammonium and sulfate ions. Nitrogen and sulfur atoms in these compounds are surrounded with a constant sphere of nearest neighbors and would thus be expected to exhibit similar atomic sensitivities from one component to the next. Similarly, the organic nitrogen and sulfur compounds are also expected to yield constant atomic sensitivities for these elements.

The second set of experiments investigated the effects of matrix dilution on photoelectron peak intensities of nitrogen and sulfur from ammonium bisulfate. Activated carbon, lead chloride, and graphite mixtures were used as the diluent matrix. As before, such mixtures were assumed to simulate the conditions normally found in atmospheric particulates.

Ammonium bisulfate was used because, along with ammonium sulfate, it is a common form of atmospheric sulfate. Since ammonium bisulfate is moderately deliquescent, it was found advantageous to first dry the substance in air at 80-90°C. This treatment resulted in an increase of S(2p)/N(1s) photoelectron peak ratio from $\sim$ 1.6 to $\sim$ 2.2, indicating the loss of ammonium. The dried ammonium bisulfate, however, was found to be stable in vacuum, both in terms of signal strength and the photoelectron peak intensity ratio.

In one series of experiments, a mixture of equal weights of Norit A activated carbon and lead chloride was used as the dilution matrix material. Samples containing different amounts of ammonium bisulfate were prepared by weighing pure substances which had been ground in an agate mortar and thoroughly mixed with a high-speed dental amalgam blender. The mixtures, containing 2, 10, 30, and 50% ammonium bisulfate, were examined by ESCA both immediately after preparation and after being exposed to laboratory air for approximately one day. The latter samples were used for the study because exposure to air allowed the ammonium bisulfate to deliquesce and perhaps more closely approximated an ambient particulate sample collected in a humid atmosphere.

The results of this dilution experiment demonstrated a constancy in the sulfate to ammonium peak ratio to within ±10%, i.e., well within the error limit for peak intensity determination.

In another dilution matrix effect study different diluents were used with a constant (dried) ammonium bisulfate concentration of 10% by weight. In addition to the activated carbon-lead chloride mixture, pure Norit A activated carbon and pure graphite powder were used as diluents. The mean value of the sulfur to nitrogen photoelectron peak intensity ratio of 2.18 ±0.30 was determined in this series of experiments. This value is within the error limits, in agreement with pure dried ammonium bisulfate.

Thus, based on these results, it seems justifiable to use relative photoelectron peak intensities to infer the apparent stoichiometry of sulfur and nitrogen containing compounds of the kind commonly associated with air pollution particulates. It will be shown later in the text that photoelectron peak intensities can be used to determine the concentration ratios of certain elements and species.

1.4.2. Binding Energy Calibration

Before outlining the results for chemical states of sulfur, nitrogen, and carbon species in atmospheric particulates, we shall first justify the use of apparent carbon (1s) binding energy to correct for sample charging. As discussed later in more detail, carbon peaks from atmospheric particulates appear essentially as a single peak with a binding energy corresponding to a neutral charge compatible with condensed hydrocarbons and/or soot-like material. Since carbon is by far the most abundant element in particulates, practically the entire ESCA C(1s) signal is due to the sample itself, rather than to hydrocarbon contamination of the sample in the spectrometer.

In order to test the validity of using the carbonaceous content of a sample as the internal binding energy reference, the apparent binding energies of C(1s) and Pb($4f_{7/2}$) from a number of ambient samples collected near a freeway were determined. The results are shown in Figure 2 where these binding energies are plotted against time of day of sample collections. (The samples were collected for 2 hours on silver membrane filters.) The figure shows that the variations in the carbon and lead peak positions are similar. Assuming that the chemical composition of lead and carbon species are similar throuout the episode, we can conclude that the binding energy error caused by the use of C(1s) as the reference should not exceed ±0.25 eV. It appears, therefore, that use of the C(1s) peak binding energy as an internal reference is adequate to determine the chemical states of major species associated with atmospheric particulates.

1.4.3. Chemical States of Sulfur and Nitrogen from Chemical Shift Measurements

The feasibility of using X-ray photoelectron spectroscopy for the chemical characterization of particulates was first explored by Novakov, Wagner, and Otvos.[37] The samples used were collected on glass fiber filters, without particle size separation, at several locations in the San Francisco Bay Area. These authors have determined the elemental composition of the particulate samples and have found that most of the particulate nitrogen is in the reduced chemical state. The observed nitrogen (1s) photoelectron lines were of complex structure, indicating the presence of several different reduced nitrogen species. The sulfur (2p) peak appeared to have a single component, consistent with sulfate.

A more systematic ESCA study of the chemical states of sulfur and nitrogen as a function of particle size and time of day was performed by Novakov et al.[2] as part of the 1969 Pasadena Smog Experiment. The particle separation was accomplished by use of a Lundgren cascade impactor. The samples for analysis were collected on Teflon films covering the rotating impactor drums. Two "size cuts," 2.0-0.6 μm and 5.0-2.0 μm, corresponding to the fourth and third impactor stages, were used in this experiment.

The sulfur (2p) spectra indicated the presence of two components which were assigned to sulfate and to sulfite. The 6+ and the 4+ state were present in both size ranges. Their relative abundance changed with particle size and time of day, however.

A more complex situation was encountered in the study of chemical states of particulate nitrogen species. The ESCA spectra from this study have revealed the presence of four different chemical states of particulate nitrogen: nitrate, ammonium, and two reduced species tentatively assigned to an amino-type and a heterocyclic nitrogen compound. Surprisingly, the nitrate was observed only in the larger particle size range but not in the smaller one.

The results just described were presented at the 161st National ACS Meeting in Los Angeles at which Hulett et al.[38] also reported on the use of ESCA for chemical characterization of coal fly ash and smoke particles. These authors have analyzed specimens of smoke particles collected on filter paper from coal burned in a home fireplace, and found three distinct components in the sulfur (2p) peak: a single reduced state assigned to a sulfide and two species of higher oxidation, corresponding

to sulfite and sulfate. The sulfur (2p) peak of fly ash particles was also found to consist of two components. These were assigned to sulfates and/or adsorbed SO_3, since their binding energies were much higher than those for sulfite ions.

Araktingi et al.[39] used ESCA to analyze particulates collected on glass fiber filters in Baton Rouge. A number of elements were identified in this work, the most abundant of which were sulfur, nitrogen, and lead. The N(1s) peak appeared to consist of at least two components with binding energies at about 399.4 and 401.5 eV. The authors did not propose an assignment to these peaks. It would appear, however, that these are similar to the nitrogen peaks identified in Pasadena samples by Novakov et al. The peak at 399.4 eV would correspond to the amino-type nitrogen, while the peak at 401.5 eV would correspond to ammonium. No appreciable nitrate was found in the study of Araktingi et al.[39] The S(2p), according to these authors, was entirely in the form of sulfate.

In summary, these early experiments have demonstrated that there is a considerable variety in the chemical states of sulfur and nitrogen associated with air pollution particulates. For example, particulate sulfur may exist in both oxidized (sulfate, adsorbed SO_3, and sulfite) and reduced (sulfide) states, while nitrogen species include nitrate, ammonium, and two other, previously unrecognized, reduced forms. This obviously suggests a more complex situation than the one inferred from wet chemical results, i.e., that the only significant sulfur and nitrogen species are sulfate, nitrate, and ammonium ions.

Craig et al.[40] have attempted to formulate an "inventory" of chemical states of particulate sulfur based on their examination of ESCA

spectra of more than a hundred samples collected at various sites in California. The samples used in that study were collected both with and without particle size segregation. All samples were collected for 2 hours as a function of time of day. The sulfur spectra of these samples were of varying degrees of complexity, sometimes covering a wide range of binding energies. The binding energies deduced from the analysis of particulate samples were assigned to certain characteristic chemical states with the help of ESCA results obtained with a number of pure compounds and with certain surface species produced by the adsorption of SO_2 and H_2S on several solids. These authors[40] caution that the chemical species were assigned in terms of reference compounds, presumably similar to those present in or on ambient particulates. This ambiguity, however, should not influence the correct assignment of major species such as sulfate, whose binding energy is not very sensitive to the choice of cations. On the other hand, it was also pointed out that species designated as adsorbed SO_3 may actually be a different compound, such as a sulfate that produces a chemical shift similar to adsorbed SO_3.

The chemical states of particulate sulfur identified in the work of Craig et al. are, in terms of the chemical shift, equivalent to adsorbed SO_3, SO_4^{--}, adsorbed SO_2, SO_3^{--}, S°, and possibly two kinds of S^{--}. The assignment of S° as neutral (elemental) sulfur was made because of the similarity of its binding energy to that of elemental sulfur. It is possible, however, that sulfur in species designated by S° is actually in the -2 oxidation state. Differences in binding energies between different sulfides are expected because of the differences in the corresponding bond ionicity. Naturally not all of these species did occur at all times

and locations. In all instances, sulfates were found to be the dominant species, although concentrations of other forms of sulfur were at times comparable to the sulfate concentrations.

As we mentioned earlier, ESCA analyses of ambient particulates uncovered the existence of previously unsuspected reduced nitrogen species[2] whose binding energies are similar to certain amines and/or heterocyclic nitrogen compounds. For simplicity we shall denote these species by N_x. Further studies on the chemical structure of N_x species were performed by Chang and Novakov[3] by means of temperature-dependent ESCA measurements. The experimental procedure consisted in measuring ESCA spectra of ambient samples and gradually increasing sample temperatures. The samples were collected on silver membrane filters which could withstand the temperatures used in the experiment.

The results of one such measurement for an ambient particulate sample, collected in Pomona, California, during a moderate smog episode (24 October 1972), are shown in Figure 3. The spectrum taken at a sample temperature of 25°C shows the presence of NO_3^-, NH_4^+, and N_x. At 80°C the entire nitrate peak is lost, accompanied by a corresponding loss in the ammonium peak intensity. The shaded portion of the ammonium peak in the 25°C spectrum represents the ammonium fraction volatilized between 25 and 80°C. The peak areas of the nitrate and the volatilized ammonium are approximately the same, indicating that the nitrate in this sample is mainly in the form of ammonium nitrate. The ammonium fraction still present at 80°C but absent at 150°C is associated with an ammonium compound more stable than ammonium nitrate, such as ammonium sulfate. At 150°C the only nitrogen species remaining in the sample is N_x. At

250°C the appearance of another peak, labeled N_x', is seen. The intensity of this peak continues to increase at 350°C. The total $N_x + N_x'$ peak area at 150, 250, and 350°C remains constant, however, indicating that a part of the N_x is transformed into N_x' as a consequence of heating.

N_x' species will remain in the sample even if its temperature is lowered to 25°C, provided that the sample has remained in vacuum. However, if the sample is taken out of vacuum and exposed to the humidity of the air, N_x' will be transformed into N_x. It was concluded that N_x' species are produced by dehydration of N_x:

$$N_x \underset{+H_2O}{\overset{-H_2O}{\rightleftharpoons}} N_x' \ .$$

Based on the described temperature behavior and on laboratory studies[3] of reactions (see below) that produce species identical to those observed in the ambient air particulates, N_x was assigned to a mixture of amines and amides. (N_x photoelectron peaks are broad indications of the presence of more than one single species.) Dehydration of the amide results in the formation of a nitrile, N_x'.

Application of temperature-dependent ESCA measurement[3,41] also revealed the presence of a hitherto unrecognized form of ammonium characterized by its relatively high volatility in vacuum. Temperature-dependent studies have also indicated that nitrate in ambient samples may occur in a volatile form different from common nitrate salts. Tentatively, such a nitrate is assigned to nitric acid adsorbed on the filter material and/or on the particles.

These conclusions are illustrated with the aid of the spectra shown in Figure 4. The spectrum shown in Figure 4a (collected in 1973 in West Covina, California) has been obtained with the sample at -150°C. The sample was kept at a low temperature in order to prevent volatile losses in the ESCA spectrometer vacuum. It will be shown later that volatilization in vacuum was suspected as one reason for the apparent inconsistency between the ammonium and nitrate determination by ESCA and by wet chemical techniques. Individual peaks corresponding to nitrate, ammonium, and N_x (amines and amides) are clearly seen in the spectrum.

Figure 4b shows the same spectral region of the same sample after its temperature was raised to 25°C. This spectrum shows only a trace of the original nitrate and about a 60% decrease in the ammonium peak intensity. Considering the nitrate and ammonium peak intensity in the lower temperature case, it is estimated that at most about 15% of the total ammonium could be associated with nitrate as NH_4NO_3. The volatile ammonium component is therefore not ammonium nitrate. Ammonium sulfate and ammonium bisulfate were found to be stable in vacuum at 25°C during time intervals normally used to complete the analysis. Furthermore, since no detectable decrease in the sulfate peak was observed over the same temperature range, it was also concluded that ammonium sulfate (and/or bisulfate) is not being volatilized in the spectrometer vacuum.

The limited volatility of ammonium salts and the behavior of the ambient samples suggests that a major fraction of ammonium in these samples is present in a previously unrecognized form. The volatility properties of nitrate in this and other samples suggest the possibility of the existence of adsorbed nitric acid in accordance with the wet chemical results of Spicer and Miller.[42]

1.4.4. Chemical Characterization of Particulate Carbon

ESCA has also been used in attempts to chemically characterize particulate carbon.[3] In most instances the carbon (1s) peak of ambient particulates appears essentially as a single peak with a binding energy compatible with either "elemental" carbon or condensed hydrocarbons or both. As seen in Figure 5, where the carbon (1s) spectrum of an ambient air particulate sample is shown, chemically shifted carbon peaks, due to suspected oxygen bonding, are of low intensity compared with the intense neutral chemical state peak.

From the standpoint of air pollution it is important to distinguish the hydrocarbon type (mostly secondary species) carbon from soot-like (primary species) carbon. Unfortunately, because of the nature of chemical bonding in hydrocarbons, these cannot be distinguished from the soot-like carbon by ESCA shift measurements under the realistic conditions of sampling and analysis.

Chang and Novakov[3] have therefore employed other supplementary measurements to estimate the relative abundance of primary particulate carbon. This was attempted by comparing the carbon (1s) peak obtained with the sample at 25°C to the carbon (1s) peak with the sample at 350°C. The difference between the low-temperature and the high-temperature runs should give the fraction of volatile carbon. Figure 5 shows the result of one such experiment for a sample collected in 1975 from West Covina. This experiment suggests that most of the ambient particulate carbon is nonvolatile in vacuum at 350°C. Assuming that the secondary hydrocarbons will have a substantial vapor pressure at 350°C, the authors have suggested

that a substantial fraction of the total particulate carbon is of a primary (soot-like) nature.

The conclusion about a high nonvolatile carbon content could be erroneous if a large fraction of particulate carbon volatilizes even at 25°C in vacuum. This seems unlikely, however, because reasonably good agreement has been found between the total carbon concentration as measured by ESCA and a combustion technique[41] (see below).

1.4.5. Chemical States of Trace Metals in Particulates

It is important to know the chemical states of trace metals in atmospheric particulates. The application of chemical shift measurements to the chemical characterization of metals has encountered difficulties because of the small differences in binding energies between different metal compounds. Chemical characterization of particulate lead species was attempted by Araktingi et al.[39] These authors have attempted to determine the relative abundance of lead oxide and lead halide in samples collected in Baton Rouge, Louisiana. Because of the small chemical shift between oxide and halide, the two suspected components could not be resolved, however. They reached the tentative conclusion that the lead in these samples is probably present as a mixture of a lead halide and an oxide.

Harker et al.[43] used ESCA to determine the chemical state of manganese in particulate emissions from a jet turbine combustion burning 2-methyl cyclopentadiene, manganese tricarbonyl (MMT) as jet fuel additive.

Manganese (3p) peak binding energies for an exhaust sample and for the compounds MnO, Mn_2O_3, Mn_3O_4, and MnO_2 were determined. These values,

corrected for sample charging using the hydrocarbon contaminant, are listed in Table I. Clearly, the oxidation state of manganese in the exhaust sample cannot be determined on the basis of chemical shift alone.

The oxidation state assignment was made by examining the multiplet splitting of the (3s) core level in the exhaust sample and some manganese compounds. In addition to oxides, MnF_2 was also studied since it is the most ionic compound of divalent manganese, and therefore its Mn^{2+} ion should exhibit the largest possible (3s) splitting. Table II gives a summary of the measured splittings along with values from the literature. In Figure 6 comparative (3s) spectra for MnF_2, exhaust particulates, and MnO_2 are shown. Based on the magnitude of the splitting, it is concluded that the oxidation state of the manganese in the combustor exhaust is +2 as MnO. Other +2 manganese compounds are eliminated by the fact that oxygen is the only negatively charged species present in sufficient concentrations to balance the manganese.

1.4.6. Quantitative Aspects of ESCA Analyses

An intermethod comparison of ESCA with analytical methods of proven accuracy and precision was undertaken by Appel et al.[41] in order to validate the quantitative aspects of ESCA analysis. This work focused on validation of sulfate, nitrate, ammonium, and carbon data as obtained by ESCA in a program to characterize ambient California particulates.

From an analytical standpoint the principal reasons for concern about the validity of ESCA analysis are:

1) Peaks in ESCA spectra corresponding to species in the same oxidation state for a given element are often poorly resolved.

2) To obtain quantitative results by ESCA, an element in the sample must be analyzed by another technique in order to provide an internal standard. For example, the ESCA analysis ratio determines the sulfate to lead peak ratio which is normalized to the lead concentration as determined by X-ray fluorescence (XRF).

3) ESCA analyzes only the surface of the exposed particles and thus may not yield analyses representative of the average composition of particles.

4) ESCA requires maintaining the sample in high vacuum, which may cause the loss of volatile species.

Samples for this study[41] were collected on 47-mm Gelman GA-1 cellulose acetate filters for sulfate analysis and on 47-mm, 1.2 μm pore size silver membrane filters for carbon and nitrogen species analysis. Two-hour samples were collected in addition to 24-hour high-volume (Whatman 41) filters.

ESCA analyses were conducted only on the membrane filters while, depending on sensitivity, wet chemical methods employed either the 2-hour or 24-hour high-volume filters. Direct comparisons involved analyses of sections from the same filters, while indirect comparison required comparison of calculated 24-hour average values from ESCA analysis of twelve 2-hour filters with the wet chemical analysis of the high-volume filter.

Three wet chemical methods[44] were used:

1) Stanford Research Institute (SRI) used a microchemical method, which measures total water-soluble sulfur, to analyze 2-hour filters.

2) Barium chloride turbidimetric analysis was used to analyze water-soluble sulfate in high-volume samples.

3) Air and Industrial Hygiene Laboratory (AIHL), California State Department of Health, uses a method for 2-hour samples which employs an excess of a barium-dye complex in acetonitrile-water solution. A decrease in absorbance due to the formation of barium sulfate is measured.

ESCA analysis included the determination of relative concentrations of sulfate and lead from the measured peak areas corrected for elemental sensitivity. Relative concentrations were converted to $\mu g/m^3$ of sulfate by normalization to lead concentration (in $\mu g/m^3$) which were determined by XRF analysis.[45]

Table III lists the results of the comparisons of ESCA sulfate determinations with those by the SRI and AIHL methods and by the $BaCl_2$ turbidimetric method. The ratio of means between wet chemical methods and ESCA varies from 0.5 to 1.0. It was concluded that ESCA provides sulfate analyses which are correct within a factor of 2. A qualitative indication of the precision of ESCA results is obtained by comparing the diurnal patterns for sulfate determined both by ESCA and by alternate procedures. Figure 7 shows sulfate diurnal patterns as measured by ESCA and by the SRI method. The data are for a 24-hour sampling period during a moderate smog episode in Pomona, California. ESCA and SRI procedures yield strikingly similar diurnal patterns suggesting a sufficient precision for the ESCA method.

More recently, Harker[46] compared the results of ESCA sulfate analysis to the results obtained by XRF and a wet chemical method. A number of 4-hr samples were collected in the Los Angeles area of fluoropore filters. The results of Harker's study are shown in Figures 8 and 9. These results obviously prove that the ESCA technique can give a good representation

of the bulk composition of atmospheric particulates in spite of its surface sensitivity.

Carbon analysis by ESCA has also been validated, and the results are described in the above-mentioned paper by Appel.[41] Twenty-nine samples collected on silver membrane filters were analyzed for total carbon, both by ESCA and by a combustion technique. A mean ratio of 0.9 ±0.1 was found between the combustion method and ESCA, suggesting that average carbon analyses are reasonably accurate.

The results of ESCA analyses for nitrate were also compared with the results of wet chemical procedures conducted on the same filters and on 24-hour filters.[41] With nitrate, using both comparative wet chemical techniques, the ESCA results were lower by a factor of about 5. This result is consistent with the volatilization of adsorbed nitric acid, as discussed above.

Similarly, ESCA analyses systematically underestimate the ammonium concentrations. The reasons for this discrepancy are related to the volatility of certain ammonium species in vacuum.

1.4.7. Determination of Molecular Forms by ESCA

ESCA analysis of particulates enables not only the possibility of detection of specific ions and functional groups, but also their mutual relationship. This is achieved by the measurement of the ESCA chemical shift augmented by the determination of relative concentrations and by study of the volatility properties of certain particulate species.

The capability of ESCA for a straightforward differentiation of different forms of atmospheric sulfates was recently demonstrated by

Novakov et al.[47,48] Figure 10 shows the nitrogen (1s) and sulfur (2p) regions in ESCA spectra of two ambient samples. One was collected in West Covina, California, in the summer of 1973, and the other was collected in St. Louis, Missouri, in the summer of 1975. The peak positions corresponding to NH_4^+, $-NH_2$, and SO_4^{--} are indicated. The solid vertical bar indicates the ammonium peak intensity expected under the assumption that the entire sulfate is in the form of ammonium sulfate. Obviously, the observed ammonium content in the West Covina sample is insufficient to account for the sulfate by itself. This is in sharp contrast with the St. Louis sample where the observed ammonium intensity closely agrees with that expected for ammonium sulfate.

These results demonstrate that ammonium sulfate in the aerosols can easily be distinguished from other forms of sulfate such as the one found in the West Covina case. However, wet chemical analyses[49] performed on West Covina samples collected simultaneously with the ESCA samples resulted in ammonium concentrations substantially higher than those suggested by the ESCA measurements. As mentioned earlier, this apparent discrepancy between the two methods was subsequently explained by the volatility of some ammonium species in the ESCA spectrometer vacuum. That these volatile losses are not caused by the volatilization of ammonium sulfate is evidenced by the St. Louis case, where no volatile losses were observed. Similarly, ammonium nitrate (negligible in these samples) and ammonium bisulfate were found to be stable in vacuum during the time periods usually required to complete the analysis. Therefore, species other than these have to be responsible for the apparent loss of ammonium in vacuum.

That the volatile ammonium is not necessarily associated with sulfate or nitrate ions is illustrated by means of results[47,48] represented in Figure 11. Here the changes in the nitrogen (1s) spectrum of a sample collected in a highway tunnel are shown as a function of the sample vacuum exposure time. Obviously, the ammonium peak intensity decreases with the vacuum exposure time of the sample. The amino-type nitrogen species intensity remains constant, however. The amount of nitrate in this sample was negligible compared with ammonium. The maximum ammonium peak expected under the assumption that the entire sulfate is ammonium sulfate is indicated by the solid vertical bar in Figure 11. It is obvious, therefore, that the counterions for this ammonium are neither nitrate nor sulfate.

Figure 12 summarizes the findings about ammonium volatility in the three samples discussed above. The shaded bars at the far left of the figure indicate the expected ammonium intensity based on the assumption that all of the sulfate in the sample is in the form of ammonium sulfate. It is evident from the figure that only the St. Louis sample contains ammonium sulfate, while the West Covina and the tunnel samples contain a different kind of ammonium which volatilizes in the spectrometer vacuum.

Novakov et al.[47,48] have applied this procedure routinely to analyze a number of ambient samples. The results of such measurements for six St. Louis samples are shown in Figure 13 where the ratio of the observed ammonium peak intensity to the peak intensity expected of the ammonium in the form of ammonium sulfate is plotted as a function of the sample vacuum exposure time. From inspection of this figure, it is evident that in addition to the cases of practically stoichiometric ammonium sulfate

(samples 913 and 914), there are cases where the observed ammonium is found in excess of ammonium sulfate. The excess ammonium consists of volatile ammonium species which decay away until ammonium sulfate is the only ammonium species left (sample 917).

The anions corresponding to the volatile ammonium species cannot be identified with certainty at this time. One possibility is that these species are produced by the adsorption of ammonia on fine soot particles to form carboxyl- and hydroxyl-ammonium complexes which have been shown to have similar volatility properties to ambient particulates.[3] Another possibility is that these species could be due to ammonium halides which are also volatile in vacuum.

In conclusion, ESCA analysis of ambient samples allows for a straightforward differentiation of different forms of atmospheric sulfate and ammonium containing species. The following distinctly different cases have been identified:

1) Ammonium sulfate accounts for the entire ammonium and sulfate content of the sample.

2) Ammonium appears in concentrations above those expected for ammonium sulfate (and nitrate). The "excess" ammonium is volatile in vacuum.

3) Ammonium appears mostly in a volatile form independent of sulfate and nitrate.

1.4.8. Use of ESCA in Reaction Mechanism Studies

ESCA has also been applied to characterize the particulate products of both heterogeneous (gas-particle) and homogeneous (gas-phase) reactions

performed under laboratory conditions. The analysis of the reaction products is essential in order to assess the relevance of such reactions to the processes that actually occur in the "real" atmosphere.

The ESCA method has been most extensively used in conjunction with heterogeneous aerosol reactions, especially those involving fine combustion-generated carbonaceous (soot) particles. These particles are the inevitable products of even seemingly complete combustion. Furthermore, the chemical properties of soot particles are similar to those of activated carbon, which is a well-known catalytically and surface chemically active material. Soot particles are formed as the result of pyrolysis, polymerization, and condensation of gases and vapors produced in the incomplete combustion of fossil fuels.[50] Fine soot particle diameters are of the order of 100 Å. The crystallites consist of several layers which exhibit the hexagonal graphitic structure.

In addition to carbon, soot particles contain about 1 to 3% hydrogen and 5 to 15% oxygen by weight.[51] Oxygen associated with soot particles is located in surface carbon-oxygen complexes, typically of the carboxyl, phenolic hydroxyl, and quinone carbonyl type.[52] The nature and the abundance of these surface complexes depend upon the combustion regime. Therefore, soot particles from different sources may differ not only in their physical properties such as size, but also in their surface chemical reactivity. An extreme case would be lamp black or carbon black. This material consists of relatively large particles and has a very low oxygen-to-carbon ratio. Fine soot particles which are invisible to the naked eye, on the other hand, have a much higher oxygen-to-carbon ratio. In this sense, fine soot particles can be regarded as an oxidized form of carbon black.

The laboratory experiments where ESCA was used to detect the reaction products involved surface chemical reactions of various carbon particles and gases such as sulfur dioxide, nitric oxide, and ammonia.

The following experiment[53] may serve as a demonstration of the oxidizing and reducing properties of carbon particles. The experiment was performed with the setup shown in Figure 14, by means of which small graphite particles (diameters ≃ 20 μm) can be collected on a filter after they have interacted with sulfur dioxide and air. The ESCA spectrum of such graphite particles clearly demonstrates the presence of two sulfur (2p) peaks corresponding to sulfate (binding energy of 168.4 eV) and sulfide. Blank filters without graphite particles, under identical sulfur dioxide exposure conditions, do not produce measurable amounts of sulfate (or sulfide).

An insight into what governs the oxidative and reductive properties of carbon particles can be gained from the results of the following experiments.[54] We have observed that the ESCA spectrum of "atomically" clean graphite (i.e., showing no trace of oxygen on its surface) exposed to about 10^{-6} torr-sec sulfur dioxide reveals only the presence of reduced sulfur species (sulfide). However, if the graphite surface were initially oxygenated and subsequently exposed to sulfur dioxide under similar conditions, sulfate formation occurred. The oxidation (or oxygenation) can be achieved by in-situ exposure of a hot graphite surface to water vapor or by cutting the graphite in air to expose the fresh surface to oxygen and moisture. These results indicate that surface carbon-oxygen complexes are responsible for the oxidative catalytic activity of carbonaceous materials. The sulfide species, on the other hand, could be produced by chemisorption of sulfur dioxide on carbon surface.

Sulfur dioxide oxidation by soot particles is demonstrated by the following experiment.[53] Soot specimens from a premixed propane-oxygen flame were prepared on silver membrane filters. In order to assure the equivalency of soot substrates to be used for experiments with different sulfur dioxide exposure conditions, small sections of each filter were cut and used in the apparatus shown in Figure 15 (insert). Dry and prehumidified particle-free air or nitrogen was used with a sulfur dioxide concentration of about 300 ppm and an exposure time of 5 min. The entire chamber was kept at about 150°C to prevent water condensation. Typical ESCA spectra of sulfur dioxide-exposed soot samples are shown in Figure 15. Sulfate peaks were always found to be more intense in the case of prehumidified air than in the case of dry air. Blank filters without soot particles exposed to sulfur dioxide and prehumidified air under identical conditions showed negligible sulfate levels. When dry and prehumidified nitrogen were used instead of air, very low levels of sulfate were produced. This indicates the importance of the oxygen in air for sulfur dioxide oxidation. Water molecules enhance the observed sulfate concentration in the air + sulfur dioxide + soot system. The only possible competing mechanism of relevance to the described experiment is sulfur dioxide oxidation via dissolved molecular oxygen in water droplets. This alternative is ruled out by the experiment with blank filter and prehumidified air, which does not result in significant sulfate formation. Furthermore, the elevated temperature prevents the formation of liquid water droplets.

The above-described experiment is a "static" experiment, i.e., with soot particles precollected on a filter and subsequently exposed to SO_2

and air. Demonstration of SO_2 oxidation on soot particles can also be done with a flow system, where SO_2 can be introduced downstream from the flame.

Photoelectron spectra representing the sulfur (2p) and carbon (1s) regions of propane soot particles produced by a Bunsen burner[48] are shown in Figure 16a. The S(2p) photoelectron peak at a binding energy of 169 eV corresponds to sulfate. The C(1s) peak appears essentially as a single component line and corresponds to a substantially neutral charge state consistent with the soot structure. It is of interest to note that even the combustion of very low sulfur content fuels (0.005% by weight) results in the formation of an easily detectable sulfate emission.

The specific role of soot particles as a catalyst for the oxidation of SO_2 is demonstrated with the aid of Figure 16b. Here we show the S(2p) and C(1s) photoelectron peaks of soot particles, generated in an analogous manner, but exposed to additional SO_2 in a flow system. A marked increase in the sulfate peak intensity, relative to carbon, is evident. The atomic ratios of sulfur to carbon in Figures 5a and 5b are about 0.15 and 0.50 respectively.

The sulfate associated with soot particles is water soluble and contributes to the acidification of the solution. These suggest that this sulfate is actually surface-bonded sulfuric acid. The hydrolysis product of this sulfate behaves chemically as sulfuric acid because it easily forms ammonium sulfate in reaction with gaseous ammonia.[48] This is illustrated in Figure 17. Figure 17a shows the N(1s) and S(2p) ESCA regions of a soot sample exposed to SO_2. Here again, the solid bar represents the ammonium intensity expected if the entire sulfate were

ammonium sulfate. The nitrogen content of this sample is low compared with sulfate. In Figure 17b the ESCA spectrum of a soot sample exposed first to SO_2 and subsequently to NH_3 in humid air is shown. It is obvious that ammonium sulfate is the principal form of sulfate in the sample.

ESCA was also used to study the formation of reduced particulate nitrogen by gas-particle reactions. It was shown that reduced nitrogen species identical to those observed in ambient particulates, i.e., N_x and a volatile ammonium species, can be produced by surface reactions of common pollutant gases such as ammonia and nitric oxide with soot particles.[3] Nitrogen species produced in these reactions at elevated temperature occur in the form of surface complexes such as amines, amides, and nitriles. Ammonium ions may be associated with soot particles in the form of carboxyl-ammonium, hydroxyl-ammonium salts, and/or physically adsorbed ammonia species produced by soot-NH_3 and soot-NO reactions at ambient temperature.

The temperature-dependent ESCA measurements of "synthetic" samples demonstrated that the nitrogen species produced by the above reactions are equivalent to the ambient air particulate species. The procedure employed is the same as that used for ambient samples.

Results in Figure 18 show that N_x species produced by surface reactions of hot soot with NH_3 have the same kind of temperature dependence as the ambient samples. The spectrum taken at room temperature shows that most nitrogen species in this sample are of the N_x type. Heating the sample in vacuum to 150°C does not influence the line shape or intensity. At 250°C, however, the formation of N_x' is evident. Further transformation of N_x to N_x' occurred at 350°C.

Synthetic N_x' species will remain unaltered even when the temperature is lowered back to room temperature if the sample remains in vacuum. However, if the sample is taken out of vacuum and exposed to moisture, N_x' will be transformed back to the original N_x compound. The behavior of the synthetic N_x species is thus identical with the behavior of ambient species.

It was proposed that at ambient temperatures surface carboxyl and phenolic groups will react with ammonia to form carboxyl ammonium or phenolic ammonium salts. Ammonia may also physically adsorb by hydrogen bonding to these same functional groups.

At elevated temperatures ammonia will react by a nucleophilic substitution reaction with carboxyl groups to produce an amide, which may become a nitrile by further dehydration. Alternatively, carboxyl and phenolic hydroxyl ammonium salts may dehydrate at elevated temperatures to produce amides and/or nitriles, and amines, respectively.

REFERENCES

1. For the principles of the ESCA method see Ref. 23. For the application of the method to the chemical characterization of particulates see T. Novakov, in: Proceedings of the Second Joint Conference on Sensing Environmental Pollutants, pp. 197-204, Instrument Society of America, Pittsburgh (1973). For a review of analytical applications see Ref. 35.

2. T. Novakov, J. W. Otvos, A. E. Alcocer, and P. K. Mueller, Chemical composition of photochemical smog aerosol by particle size and time of day; chemical states of sulfur and nitrogen by photoelectron spectroscopy, J. Colloid Interface Sci. 39, 225 (1972).

3. S. G. Chang and T. Novakov, Formation of pollution particulate nitrogen compounds by NO-soot and NH_3-soot gas-particle surface reactions, Atmos. Environment 9, 495 (1975).

4. C. E. Junge, Atmospheric Chemistry and Radioactivity, Academic Press, New York (1973).

5. G. M. Hidy and C. S. Burton, Atmospheric aerosol formation by chemical reactions, Int. J. of Chem. Kinetics, Symposium 1, 509 (1975).

6. T. Koopmans, Über die Zuordnung von Wellenfunktionen und Eigenwerten zu den einzelnen Elektronen eines Atoms, Physica 1, 104 (1933).

7. P. S. Bagus, Self-consistent field wave functions for hole states of some Ne-like and Ar-like ions, Phys. Rev. 139, A619 (1965).

8. A. Rosen and I. Lindgren, Relativistic calculations of electron binding energies by a modified Hartree-Fock-Slater method, Phys. Rev. 176, 114 (1968).

9. M. E. Schwartz, Direct calculation of binding energies of inner-shell electrons in molecules, Chem. Phys. Lett. 5, 50 (1970).

10. C. R. Brundle, M. B. Robin, and H. Basch, Electronic energies and electronic structures of the fluoromethanes, J. Chem. Phys. 53, 2196 (1970).

11. P. Siegbahn, Ab initio calculations on furan with a new computer program, Chem. Phys. Lett. 8, 245 (1971).

12. L. Hedin and G. Johansson, Polarization corrections to core levels, J. Phys. B 2, 1336 (1969).

13. L. C. Snyder, Core-electron binding energies and Slater atomic shielding constants, J. Chem. Phys. 55, 95 (1971).

14. D. Liberman, Improvement on Koopmans' theorem, Bull. Am. Phys. Soc. Ser. 9, 731 (1964).

15. R. Manne and T. Aberg, Koopmans' theorem for inner-shell ionization, Chem. Phys. Lett. 7, 282 (1970).

16. T. D. Thomas, X-ray photoelectron spectroscopy of halomethanes, J. Am. Chem. Soc. 92, 4184 (1970).

17. K. Siegbahn, C. Nordling, G. Johansson, J. Hedman, P. F. Heden, K. Hamrin, U. Gelius, T. Bergmark, L. O. Werme, R. Manne, and Y. Baer, ESCA Applied to Free Molecules, North-Holland, Amsterdam (1969).

18. M. E. Schwartz, Correlation of core electron binding energies with the average potential at a nucleus: carbon 1s and extended Hückel theory valence molecular orbital potentials, Chem. Phys. Lett. 7, 78 (1971).

19. J. A. Pople, D. P. Santry, and G. P. Segal, Approximate self-consistent molecular orbital theory. I. Invariant procedures, J. Chem. Phys. 43, S129 (1965).

20. F. O. Ellison and L. L. Larcom, ESCA: a new semi-empirical correlation

between core-electron binding energy and valence-electron density, Chem. Phys. Lett. 10, 580 (1971).

21. D. W. Davis, D. A. Shirley, and T. D. Thomas, K-electron binding energy shifts in fluorinated methanes and benzenes: comparison of a CNDO potential method with experiment, J. Chem. Phys. 56, 671 (1972).

22. U. Gelius, P. F. Heden, J. Hedman, B. J. Lindberg, R. Manne, R. Nordberg, C. Nordling, and K. Siegbahn, Molecular spectroscopy by means of ESCA, Phys. Ser. 2, 70 (1970).

23. U. Gelius, B. Roos, and P. Siegbahn, Ab initio MO SCF calculations of ESCA shifts in sulphur-containing molecules, Chem. Phys. Lett. 4, 471 (1970).

24. K. Siegbahn, C. Nordling, A. Fahlman, R. Nordberg, K. Hamrin, J. Hedman, G. Johansson, T. Bergmark, S.-E. Karlsson, I. Lindgren, and B. J. Lindberg, ESCA—atomic, molecular and solid state structure by means of electron spectroscopy, Nova Acta Regiae Soc. Sci. Upsaliensis Ser. IV, Vol. 20 (1967).

25. H. Basch, On the interpretation of K-shell electron binding energy

chemical shifts in molecules, Chem. Phys. Lett. 5, 337 (1970).

26. M. E. Schwartz, Correlation of 1s binding energy with the average quantum mechanical potential at a nucleus, Chem. Phys. Lett. 6, 631 (1970).

27. C. S. Fadley, Multiplet splittings in photoelectron spectra, in: Electron Spectroscopy (D. A. Shirley, ed.), p. 781, North-Holland, Amsterdam (1972).

28. See C. S. Fadley, R. Baird, W. Siekhaus, T. Novakov, and S. A. L. Bergstrom, Surface analysis and angular distribution measurements in X-ray photoelectron spectroscopy, J. Electron Spectroscopy 4, 93 (1974) and references therein.

29. C. D. Wagner, Sensitivity of detection of the elements by photoelectron spectrometry, Anal. Chem. 44, 1050 (1972).

30. R. S. Swingle II, Quantitative surface analysis by X-ray photoelectron spectroscopy, Anal. Chem. 47, 21 (1975).

31. D. M. Wyatt, J. C. Carver, and D. M. Hercules, Some factors affecting the application of electron spectroscopy (ESCA) to quantitative analysis of solids, Anal. Chem. 47, 1297 (1975).

32. P. E. Larson, Quantitative measurements on gold-silver alloys by X-ray photoelectron spectroscopy, Anal. Chem. 44, 1678 (1972).

33. W. E. Swartz, Jr., and D. M. Hercules, X-ray photoelectron spectroscopy of molybdenum compounds. Use of electron spectroscopy for chemical analysis (ESCA) in quantitative analysis, Anal. Chem. 43, 1774 (1971).

34. C. R. Brundle and M. W. Roberts, Surface sensitivity of ESCA [electron spectroscopy for chemical analysis] for submonolayer quantities of mercury adsorbed on a gold substrate, Chem. Phys. Lett. 18, 380 (1973).

35. D. M. Hercules and J. C. Carver, Electron spectroscopy: X-ray and electron excitation, Anal. Chem. 46, 133R (1974).

36. J. S. Brinen, Applying electron spectroscopy for chemical analysis to industrial catalysis, Accounts Chem. Res. 9, 86 (1976).

37. T. Novakov, C. D. Wagner, and J. W. Otvos, Analysis of atmospheric particulates by means of a photoelectron spectrometer, paper presented at the Pacific Conference on Chemistry and Spectroscopy, Abstracts, p. 46, San Francisco, October 1970.

38. L. D. Hulett, T. A. Carlson, B. R. Fish, and J. L. Durham, Studies of sulfur compounds adsorbed on smoke particles and other solids by photoelectron spectroscopy, Proceedings of the Symposium on Air Quality, p. 179, Plenum, New York (1972).

39. Y. E. Araktingi, N. S. Bhacca, W. G. Proctor, and J. W. Robinson, Analysis of airborne particulates by electron chemistry for chemical analysis (ESCA), Spectrosc. Lett. 4, 365 (1971).

40. N. L. Craig, A. B. Harker, and T. Novakov, Determination of the chemical states of sulfur in ambient pollution aerosols by X-ray photoelectron spectroscopy, Atmos. Environment 8, 15 (1974).

41. B. R. Appel, J. J. Wesolowski, E. Hoffer, S. Twiss, S. Wall, S. G. Chang, and T. Novakov, An intermethod comparison of X-ray photoelectron spectroscopic analysis of atmospheric particulate matter, Intern. J. Environ. Anal. Chem. 4, 169 (1976).

42. D. F. Miller and C. W. Spicer, Measurement of nitric acid in smog, J. Air Poll. Control Assoc. 25, 940 (1975).

43. A. B. Harker, P. J. Pagni, T. Novakov, and L. Hughes, Manganese emissions from combustors, Chemosphere 6, 339 (1975).

44. For the description of wet chemical methods see Reference 41 and references therein.

45. R. D. Giauque, data presented in: Characterization of Aerosols in California (ACHEX), Vol. III, Science Center, Rockwell International, final report to Air Resources Board, State of California (September 1974).

46. A. B. Harker, Quantitative Comparison of the XPS Technique with XRF and Wet Chemical Sulfur Analyses, Science Center, Rockwell International, Internal Technical Report (1976); and private communication.

47. T. Novakov, R. L. Dod, and S. G. Chang, Study of air pollution particulates by X-ray photoelectron spectroscopy, Fresenius' Zeitschr. Anal. Chem., in press (1976).

48. T. Novakov, S. G. Chang, R. L. Dod, and H. Rosen, Chemical characterization of aerosol species produced in heterogeneous gas-particle reactions, APCA Paper 76-20.4, presented at the Air Pollution Control Association Annual Meeting, Portland, Oregon, June 1976. Also Lawrence Berkeley Laboratory Report LBL-5215 (June 1976).

49. C. W. Spicer, private communication.

50. J. B. Edwards, Combustion-Formation and Emission of Trace Species, Ann Arbor Science, Ann Arbor (1974), and references therein.

51. A. Thomas, Carbon formation in flames, Combustion and Flame 6, 46 (1972).

52. H. P. Boehm, Chemical identification of surface groups, Advan. Catal. Relat. Subj. 16, 179 (1966).

53. T. Novakov, S. G. Chang, and A. B. Harker, Sulfates as pollution particulates: catalytic formation on carbon (soot) particles, Science 186, 259 (1974).

54. T. Novakov and W. Siekhaus, unpublished data.

Table I. Measured Mn(3p) electron binding energies.[a]

Sample	Exhaust	MnO[b]	Mn_3O_4	Mn_2O_3	MnO_2
Binding energy (eV)	48.9 0.2	48.8 0.2	48.9 0.2	49.0 0.2	49.9 0.2

[a]From Ref. 43.

[b]Powdered reagent grade MnO which undergoes rapid surface oxidation at ambient conditions was used.

Table II. Multiplet splitting of Mn(3s).[a]

Compound	Splitting (eV)			
	This work	Wertheim et al.[b]	Fadley et al.[c]	Carver et al.[d]
MnF_2 (2+)	6.4±0.2	6.50±0.02	6.5	6.3
Exhaust particulate	6.1±0.2	—	—	—
MnO (2+)	—	6.05±0.04	5.7[e]	5.5[e]
Mn_3O_4 (2+ and 3+)	5.5±0.2	—	—	—
Mn_2O_3 (3+)	5.5±0.2	5.50±0.10	—	5.4
MnO_2 (4+)	4.6±0.2	4.58±0.06	4.6	—

[a]From Ref. 43.

[b]G. K. Wertheim, S. Hutner, and H. J. Guggenheim, Phys. Rev. B 7(1), 556 (1973).

[c]C. S. Fadley, D. A. Shirley, A. J. Freeman, P. S. Bagus, and J. V. Mallow, Phys. Rev. Lett. 23, 1397 (1969).

[d]J. C. Carver, T. A. Carlson, L. C. Cain, and G. K. Schweitzer, in: Electron Spectroscopy (D. A. Shirley, ed.), p. 803, North-Holland, Amsterdam (1972).

[e]Earlier lower values for MnO were due to surface oxidation of available analytical grade MnO. The MnO reference compound used in b) was produced by oxidation of clean Mn in vacuo.

Table III. Comparison of sulfate data, ESCA vs wet chemistry.[a]

		$\mu g/m^3$ sulfate		
		ESCA Cellulose ester filters vs $\bar{\Sigma}$ 2-hour low volume	Wet chemistry Whatman 41 24-hour hi volume	
Site	Date	Hi vol. wet chemistry	$\bar{\Sigma}$ 2-hr low vol. ESCA	Hi vol./ $\bar{\Sigma}$ 2-hr low vol.
San Jose	8-17-72	1.6±0.4	1.1±0.2	1.5±0.5
San Jose	8-21-72	1.0±0.2	1.4±0.3	0.7±0.2
Fresno	8-31-72	4.2±1.0	4.0±1.1	1.1±0.4
Riverside	9-19-72	5.9±1.5	6.4±4.6	0.9±0.7
Ratio of means = 1.0				
Spearmans ρ = 0.80				
Linear regression slope = 1.0 (intercept $\equiv$ 0)				

[a]From Ref. 1.

FIGURE CAPTIONS

Figure 1. Intensity ratios of sulfur (2p) and nitrogen (1s) photoelectron peaks, corrected for stoichiometry, for a number of pure sulfur and nitrogen containing compounds.

Figure 2. Apparent binding energies (not corrected for sample charging) of carbon (1s) and lead ($4f_{7/2}$) photoelectrons from a number of 2-hour samples collected near a freeway. The apparent binding energies are plotted against time of day corresponding to sample collection.

Figure 3. Nitrogen (1s) photoelectron spectrum of an ambient sample as measured at 25, 80, 150, 250, and 350°C (from Ref. 3).

Figure 4. a) Nitrogen (1s) photoelectron spectrum of an ambient sample as measured at -150°C.

b) The spectrum of the same sample as measured at 25°C (from Ref. 3).

Figure 5. Carbon (1s) photoelectron spectrum of an ambient sample as measured at 25 and 350°C. The shaded area represents the difference between low and high temperature spectra. The apparent volatile losses are mainly confined to the chemically shifted component of the carbon peak (from Ref. 3).

Figure 6. Manganese (3s) spectra of MnF_2, exhaust particles, and MnO_2 showing the multiplet splitting of the 3s core level (from Ref. 43).

Figure 7. Diurnal variations of sulfate as measured by ESCA and by a wet chemical method (SRI). The data are for a 24-hour sampling period during a smog episode in southern California (from Ref. 41).

Figure 8. Comparison of quantitative particulate sulfate analyses by ESCA and X-ray fluorescence spectroscopy (from Ref. 46).

Figure 9. Comparison of quantitative particulate sulfate analyses by ESCA and a colorimetric wet chemical procedure (from Ref. 46).

Figure 10. Nitrogen (1s) and sulfur (2p) regions in X-ray photoelectron spectra of two ambient samples. The peak positions corresponding to NH_4^+, $-NH_2$ (N_x), and SO_4^{--} are indicated. The solid vertical bar represents the ammonium intensity expected under the assumption that the entire sulfate is in the form of ammonium sulfate. The difference in the relative ammonium content of the two samples is obvious. The sulfate and ammonium intensities in the St. Louis sample are compatible with ammonium sulfate. The ammonium content in the West Covina sample is insufficient to be compatible with ammonium sulfate. Both samples were exposed to the spectrometer vacuum for about one hour (from Ref. 48).

Figure 11. The variation in the observed ammonium peak intensity with vacuum exposure for a sample collected in a highway tunnel. The decrease in the peak intensity is caused by the volatilization of the ammonium species present in the sample. The solid vertical bar represents the ammonium intensity expected under the assumption that the sulfate in this sample is in the form of ammonium sulfate. The nitrate in this sample is also small compared to ammonium. The ammonium in this sample is considerably in excess of that expected for ammonium sulfate or ammonium nitrate (from Ref. 48).

Figure 12. Volatility properties of West Covina, St. Louis, and automotive ammonium aerosol. The shaded bars on the far left of the figure indicate the expected ammonium intensity if the entire sulfate were ammonium sulfate (from Ref. 48).

Figure 13. Volatility property of ammonium in six ambient St. Louis samples. The ratio of the observed ammonium peak to the one expected under the assumption that the entire sulfate in these samples is ammonium sulfate vs vacuum exposure time is shown. Note the cases of apparently stoichiometric ammonium sulfate (samples 913 and 914) and the cases where the volatile ammonium component is found in excess of that required for ammonium sulfate (from Ref. 48).

Figure 14. Experimental arrangement used to study the interaction of SO_2 with graphite particles. The rotation of the stainless steel rotor produces small graphite particles, which can be collected on a filter after they have interacted with SO_2. The ESCA spectrum of graphite particles reveals two sulfur (2p) peaks corresponding to sulfate and to sulfides (from Ref. 53).

Figure 15. Apparatus used to study the interaction of SO_2 with soot particles collected on filters from a propane-oxygen flame. Dry or prehumidified particle-free air was used. Typical ESCA spectra of SO_2-exposed soot are also shown. Sulfate peaks were found to be always more intense in the case of prehumidified air. Blank filters, that is, filters without soot particles, exposed to SO_2 and prehumidified air under identical conditions showed only low, background-level sulfate peaks (from Ref. 53).

Figure 16. Carbon (1s) and sulfur (2p) photoelectron spectrum of:

a) Soot particles produced by combustion of propane saturated with benzene vapor. The sulfur content of this fuel is 0.005% by weight.

b) Soot particles generated in an analogous manner to a), but exposed to additional SO_2 in humid air (from Ref. 48).

Figure 17. a) ESCA spectrum of sulfate produced by catalytic oxidation of SO_2 on soot particles. Note that the nitrogen content in this sample is low compared with sulfate.

b) ESCA spectrum of a soot sample exposed first to SO_2 (i.e., as in Fig. 16a), and subsequently to NH_3 in humid air. Formation of ammonium sulfate is evident.

Figure 18. Nitrogen (1s) spectrum of a soot sample exposed to NH_3 at elevated temperature as measured at 25, 150, 250, and 350°C (from Ref. 3).

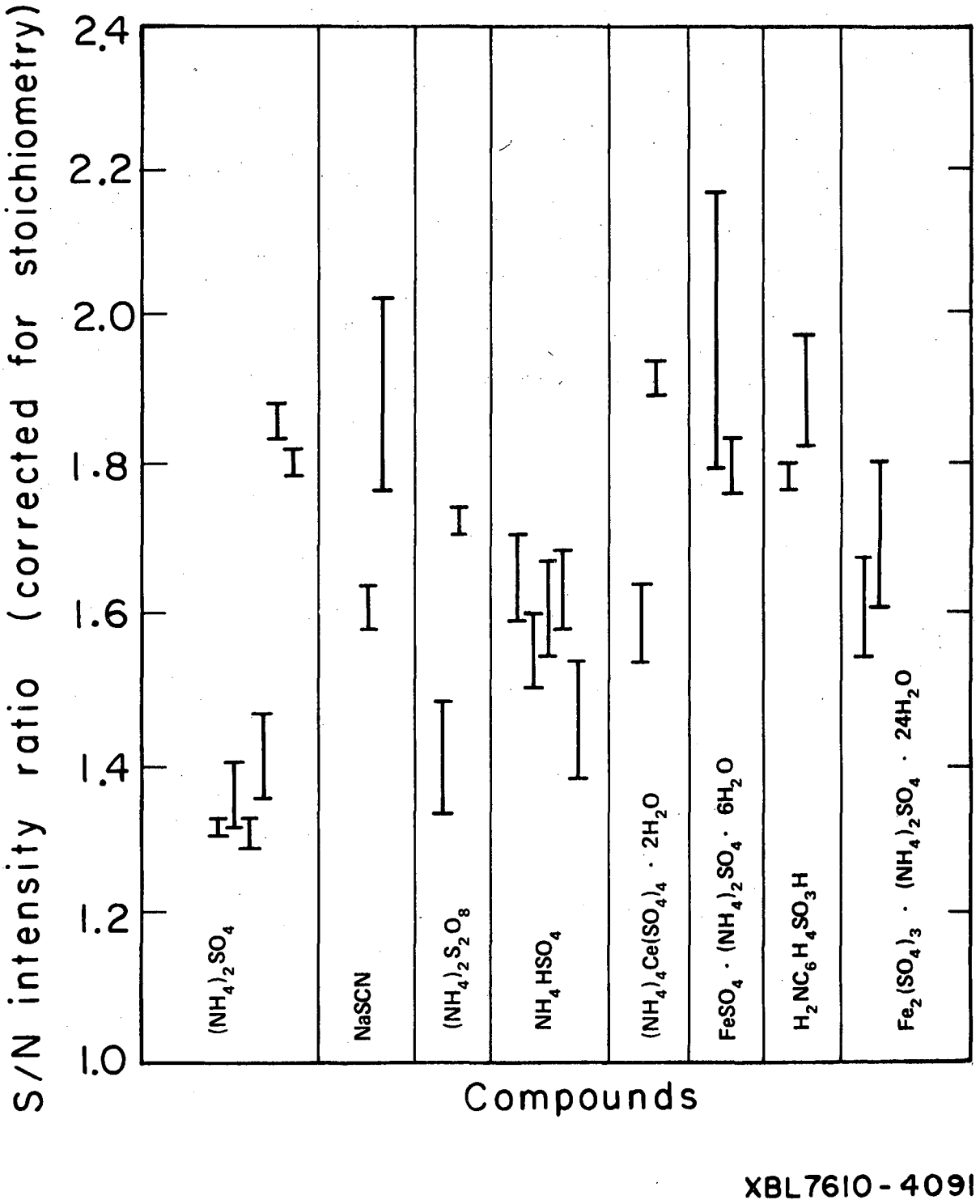
S/N intensity ratio (corrected for stoichiometry)
2.4
2.2
2.0
1.8
1.6
1.4
1.2
1.0
$(NH_4)_2SO_4$
NaSCN
$(NH_4)_2S_2O_8$
NH_4HSO_4
$(NH_4)_4Ce(SO_4)_4 \cdot 2H_2O$
$FeSO_4 \cdot (NH_4)_2SO_4 \cdot 6H_2O$
$H_2NC_6H_4SO_3H$
$Fe_2(SO_4)_3 \cdot (NH_4)_2SO_4 \cdot 24H_2O$
Compounds
XBL7610-4091

Figure 1

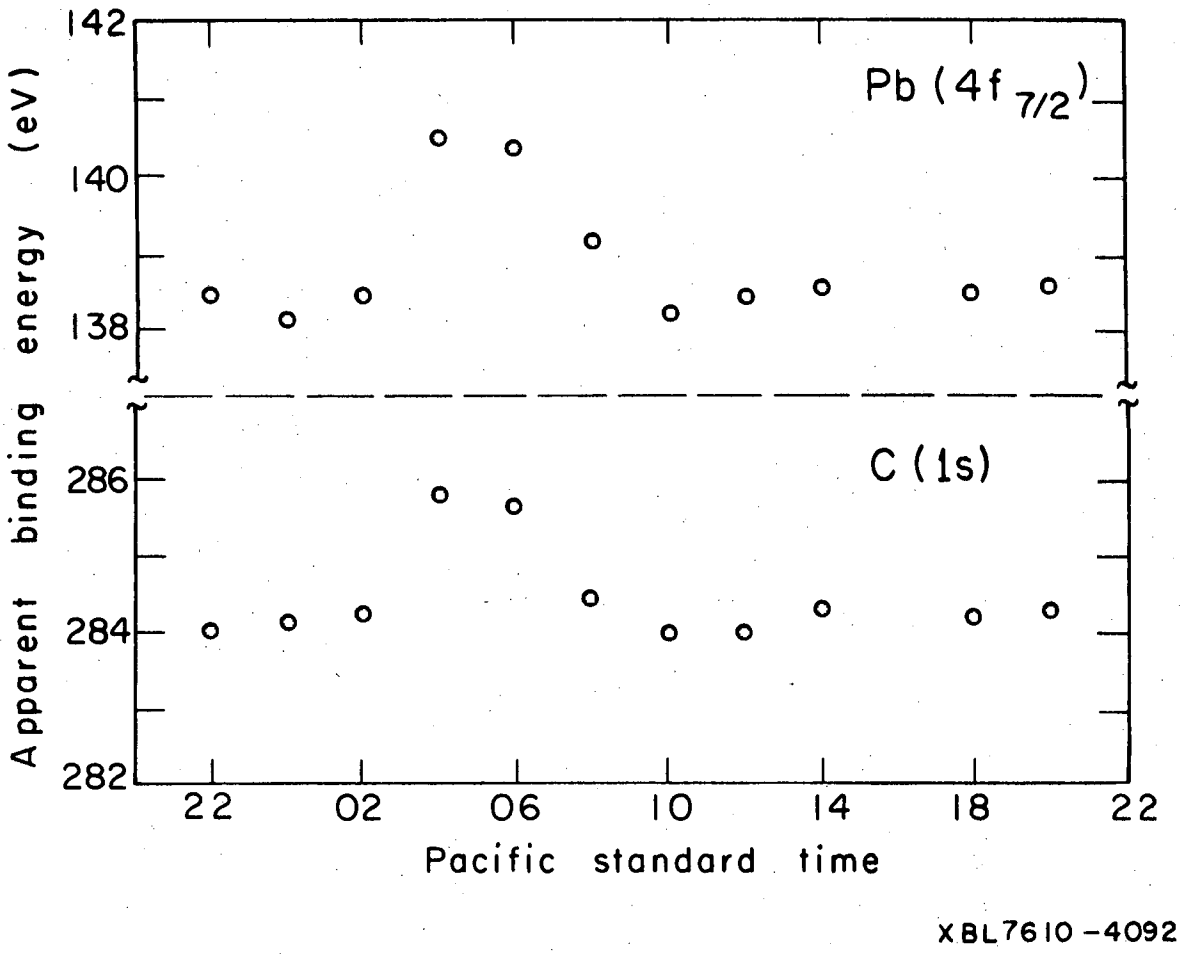

Figure 2

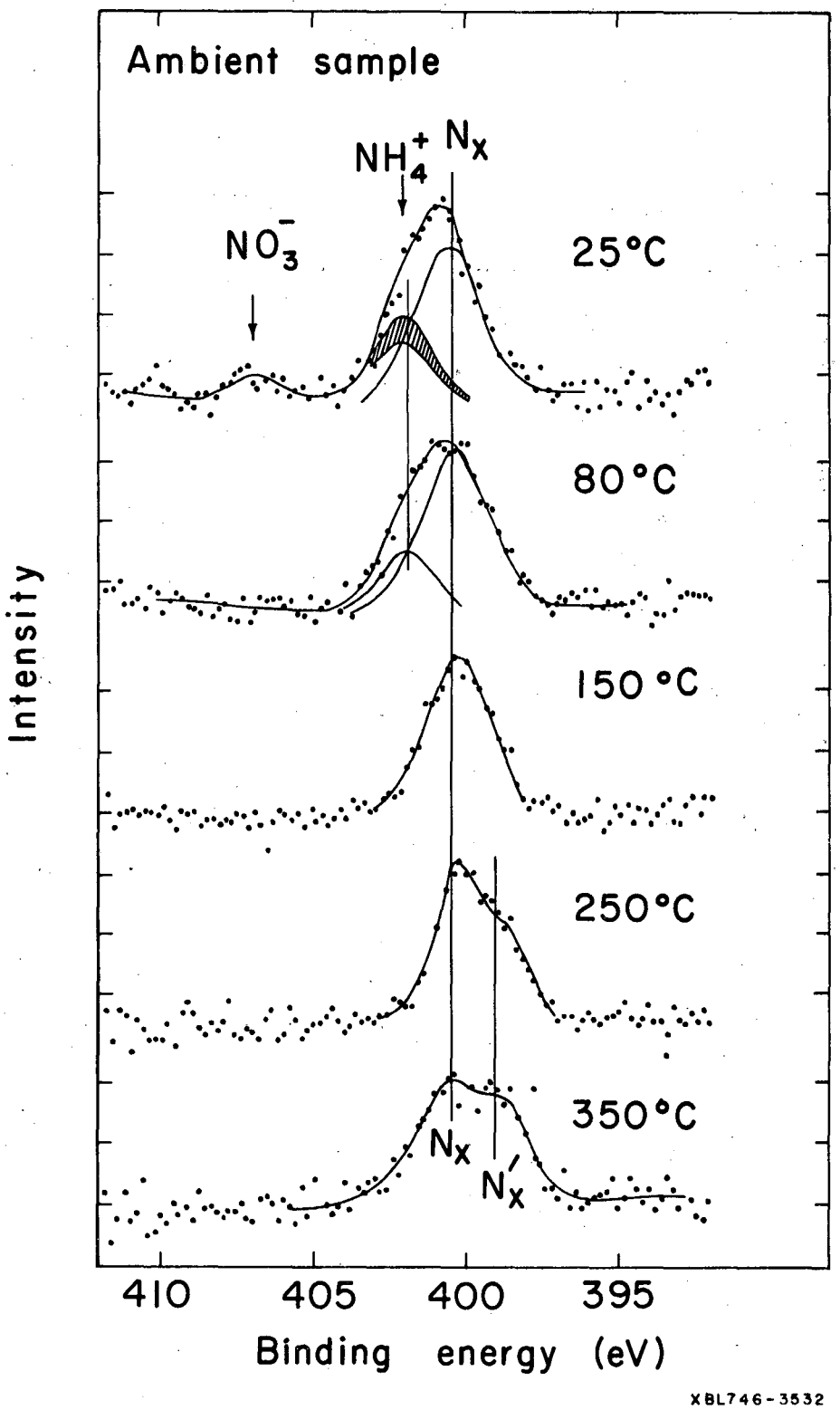
Ambient sample
NH_4^+ N_x
NO_3^-
25°C
80°C
150°C
250°C
350°C
N_x
N_x'
Intensity
410
405
400
395
Binding energy (eV)
XBL746-3532

Figure 3

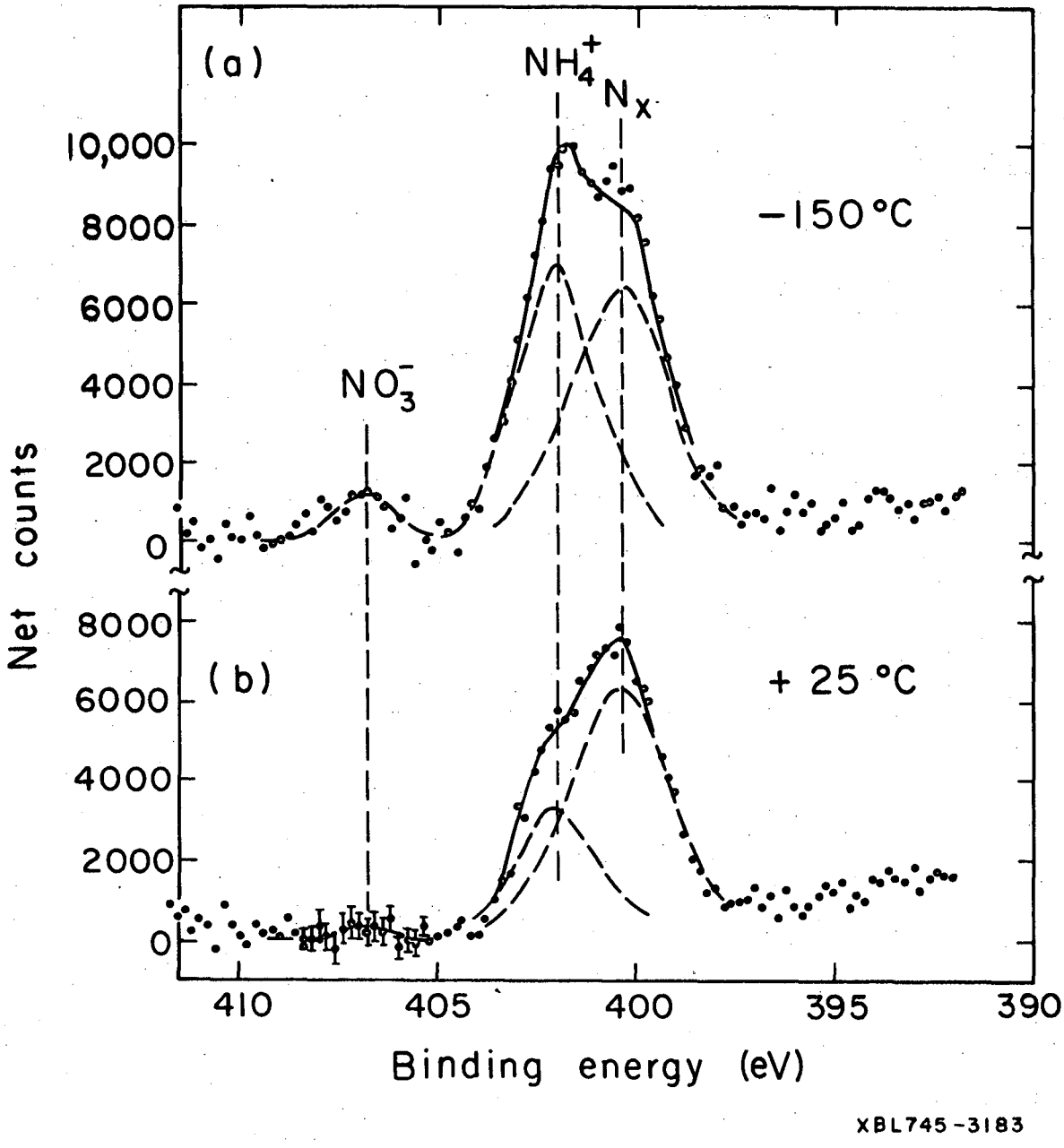

Figure 4

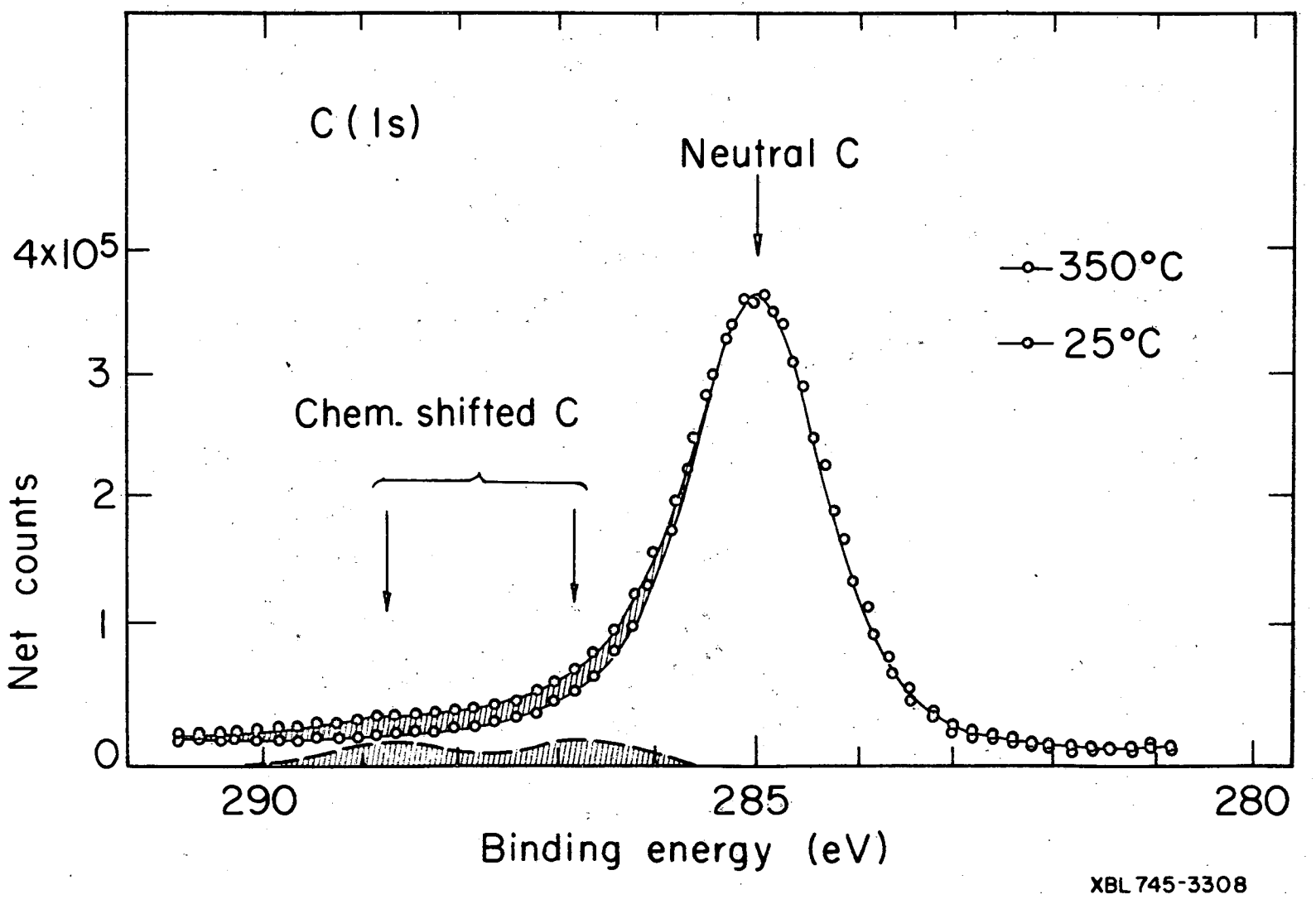

Figure 5

LBL-5278

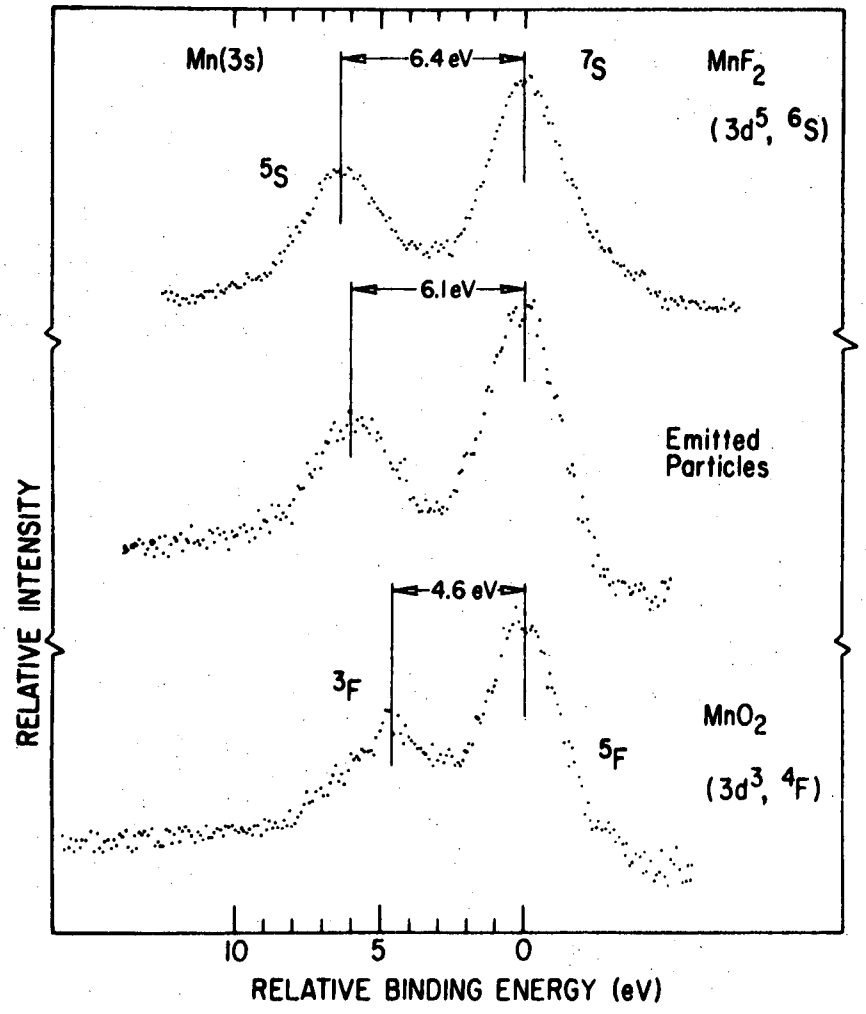

XBL 767-8541

Figure 6

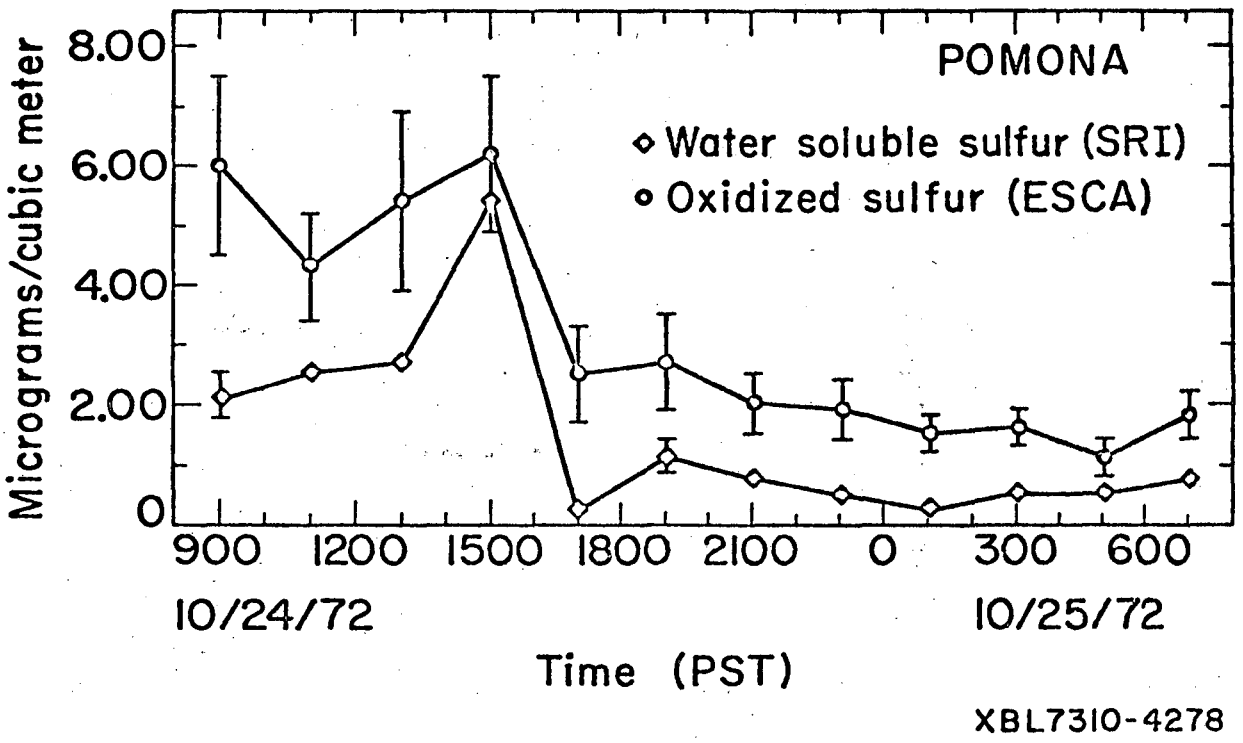
POMONA
◇ Water soluble sulfur (SRI)
○ Oxidized sulfur (ESCA)
Micrograms/cubic meter
8.00
6.00
4.00
2.00
0
900
1200
1500
1800
2100
0
300
600
10/24/72
10/25/72
Time (PST)
XBL7310-4278

Figure 7

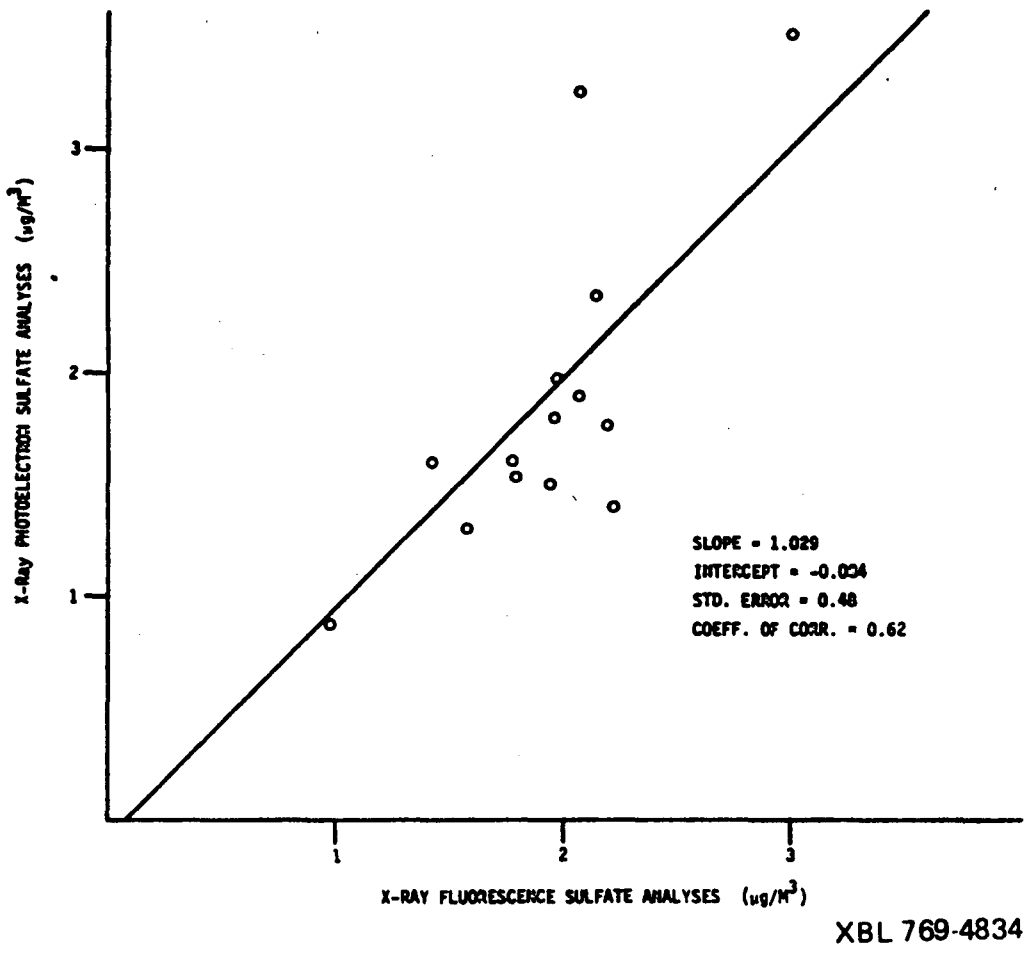

Figure 8

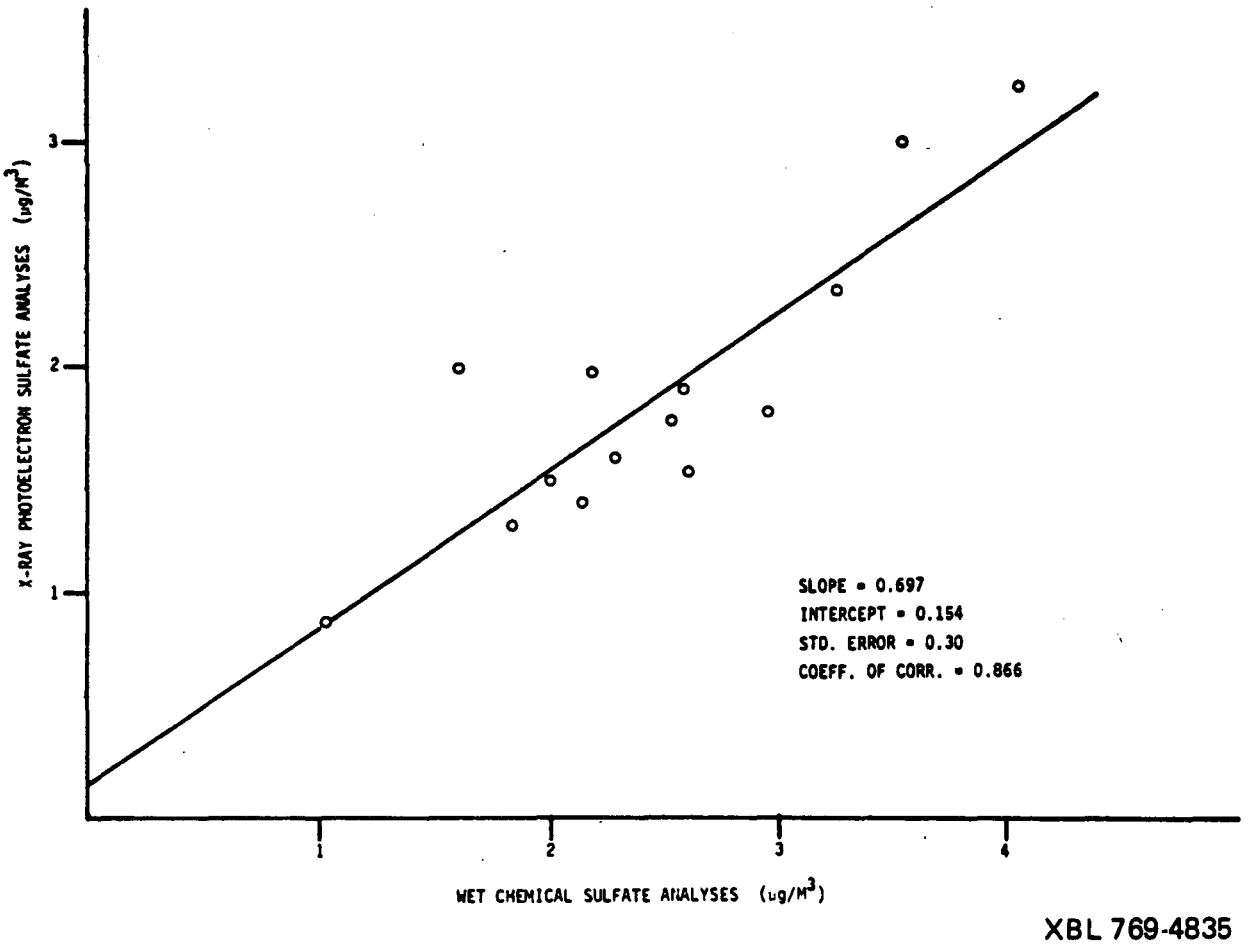

XBL 769-4835

Figure 9

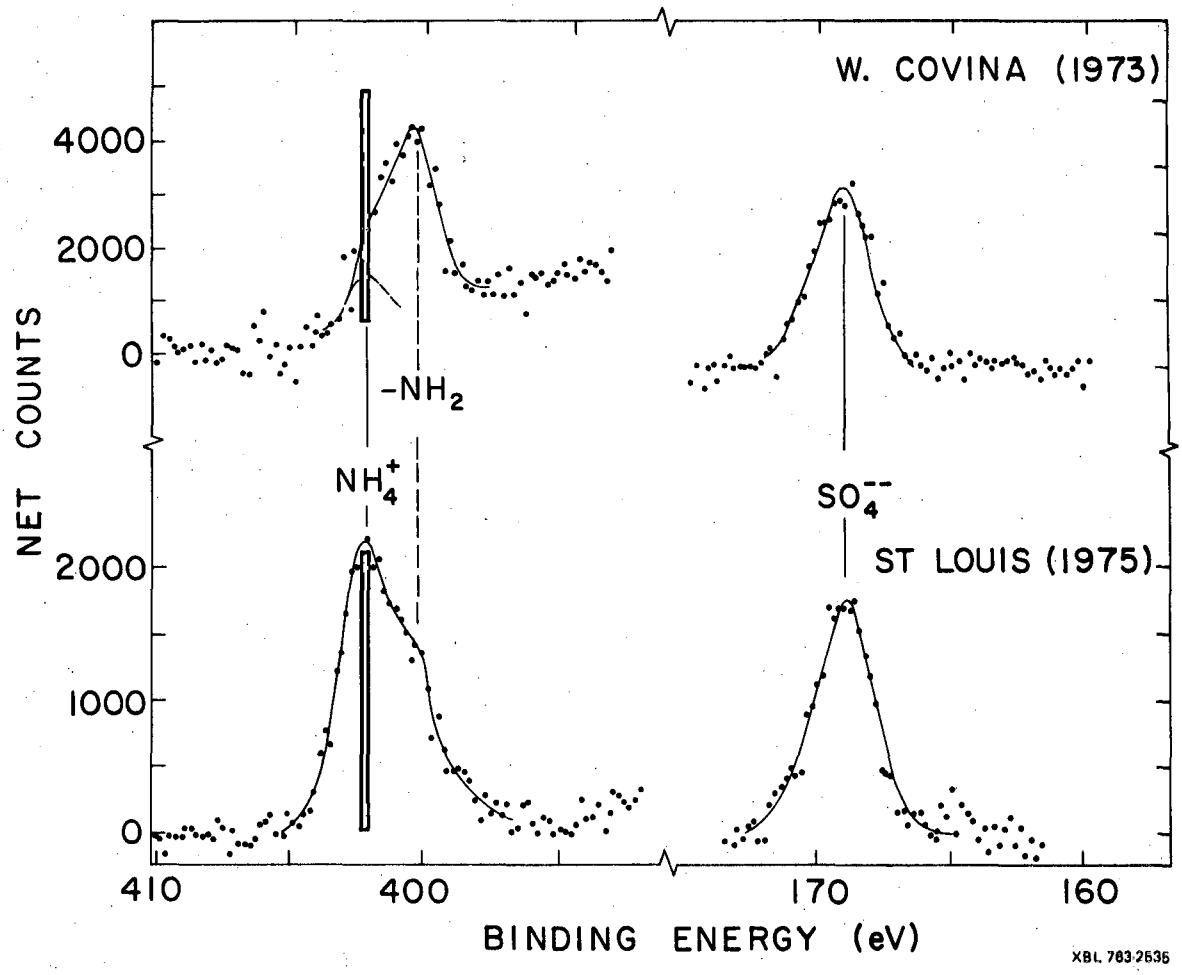

Figure 10

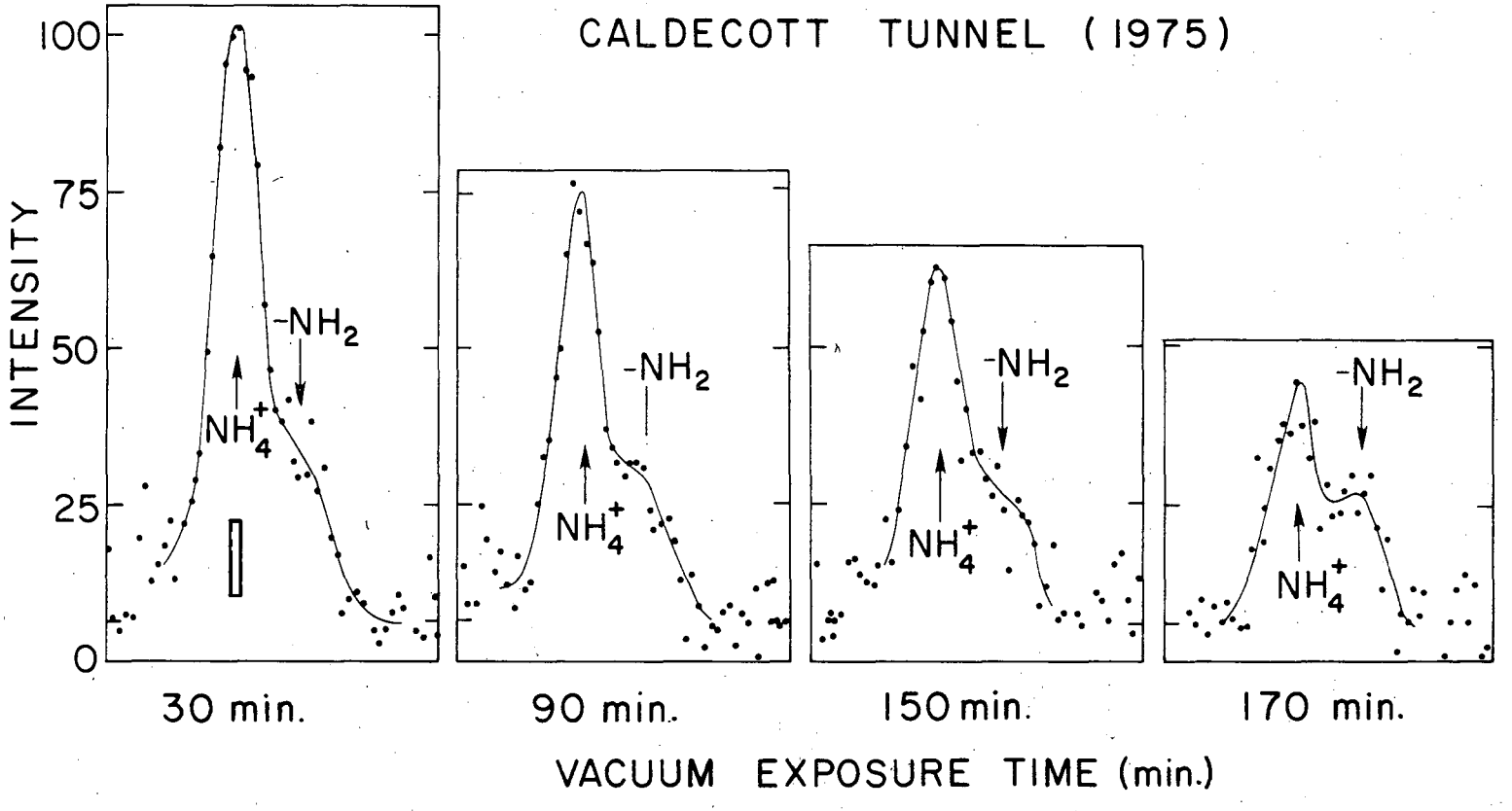
CALDECOTT TUNNEL (1975)
INTENSITY
100
75
50
25
0
-NH2
NH4+
30 min.
90 min.
150 min.
170 min.
VACUUM EXPOSURE TIME (min.)
XBL 763-2537

Figure 11

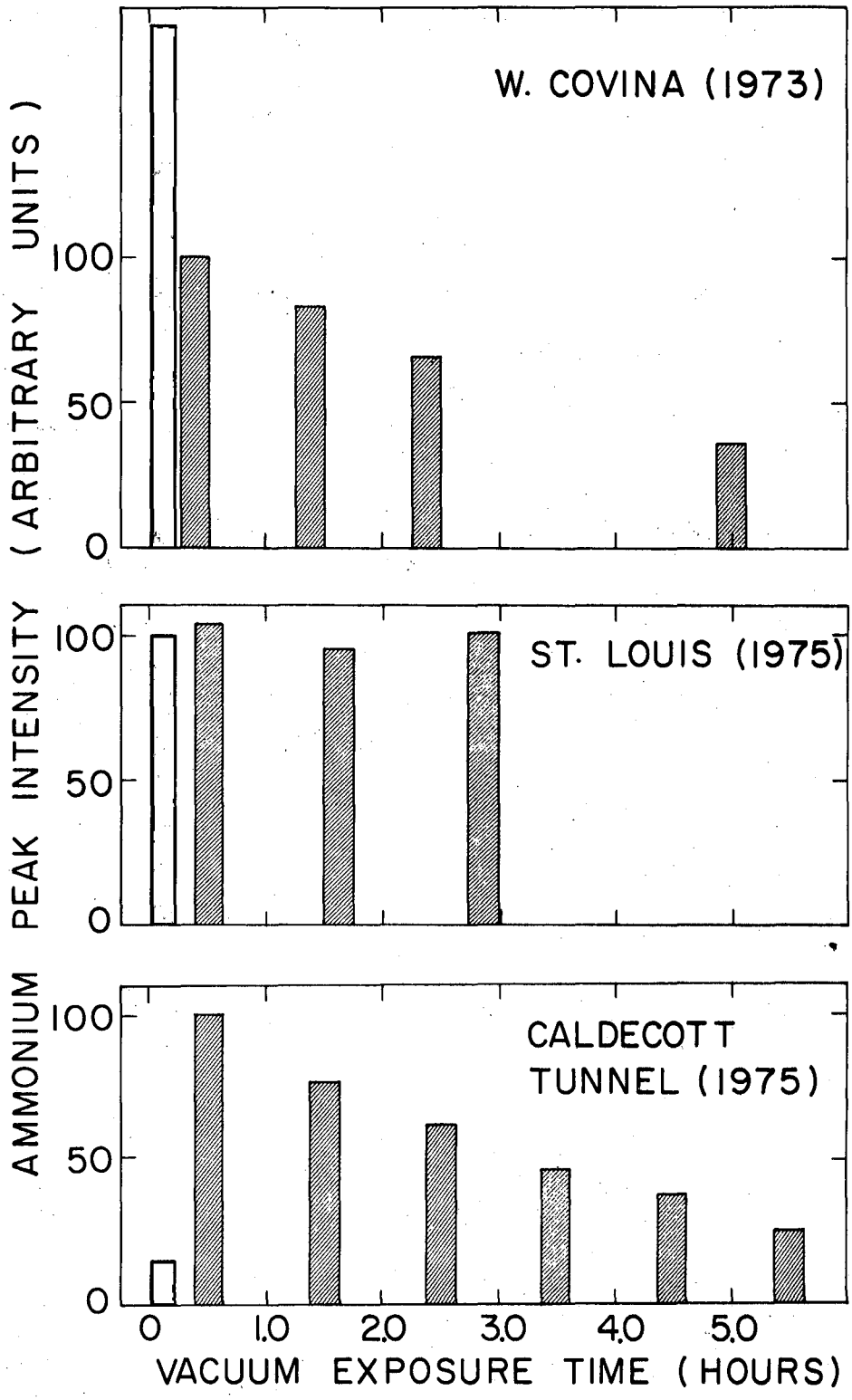

XBL 763-2536

Figure 12

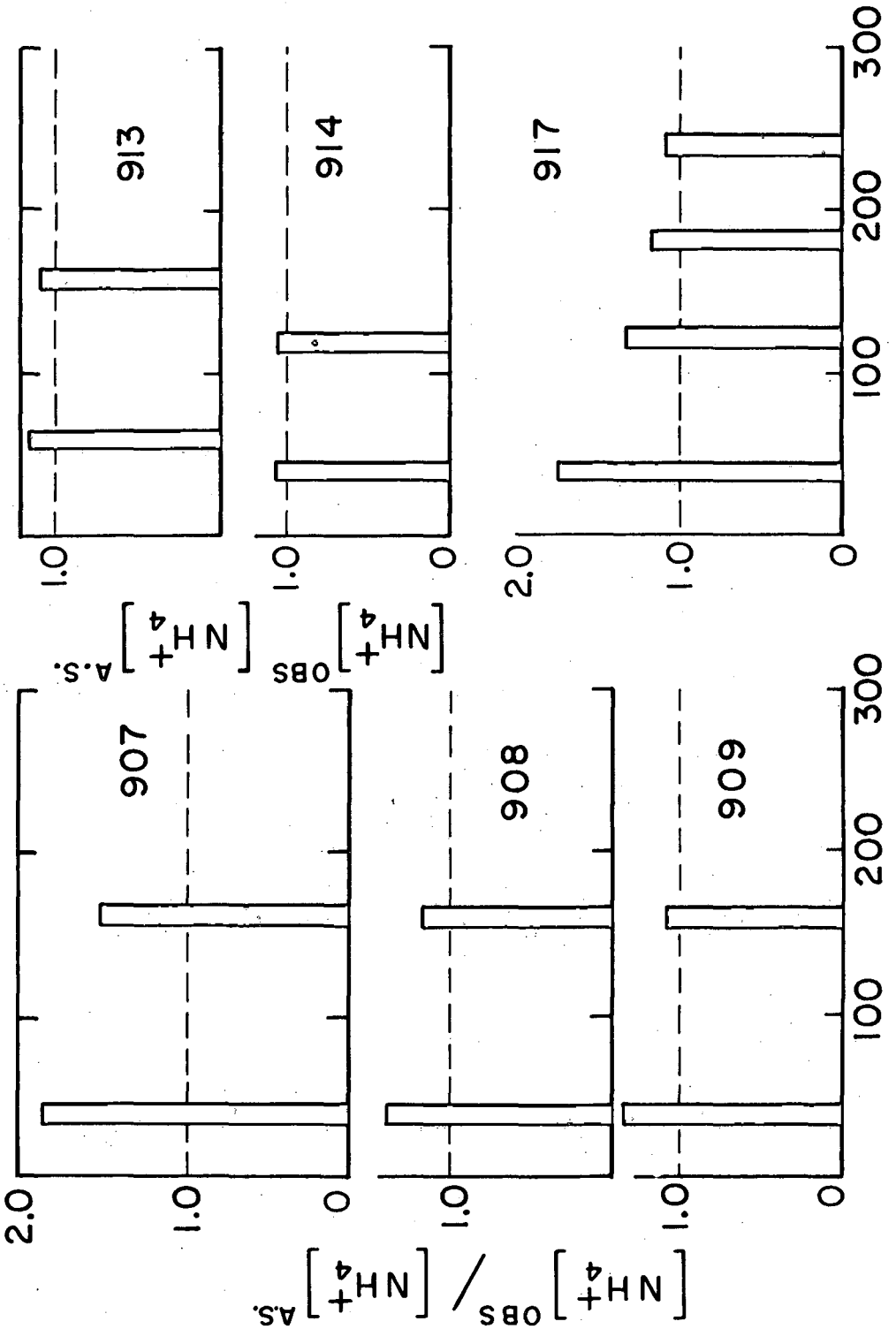
913
914
917
907
908
909
2.0
1.0
0
100
200
300
Vacuum exposure time (minutes)
$\left[NH_4^+\right]_{OBS} / \left[NH_4^+\right]_{A.S.}$
$\left[NH_4^+\right]_{OBS} \left[NH_4^+\right]_{A.S.}$
XBL 766-3049

Figure 13

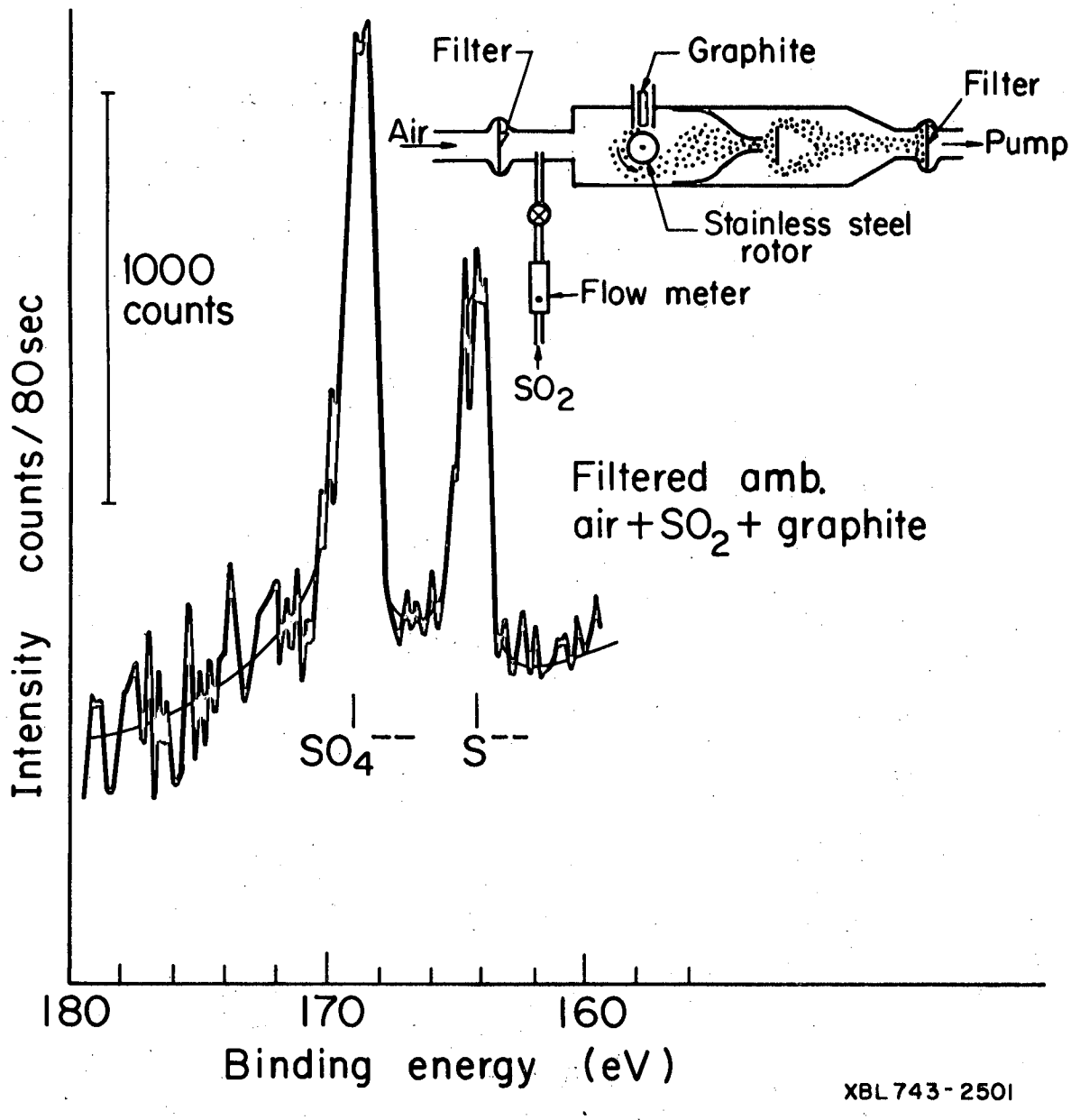

Figure 14

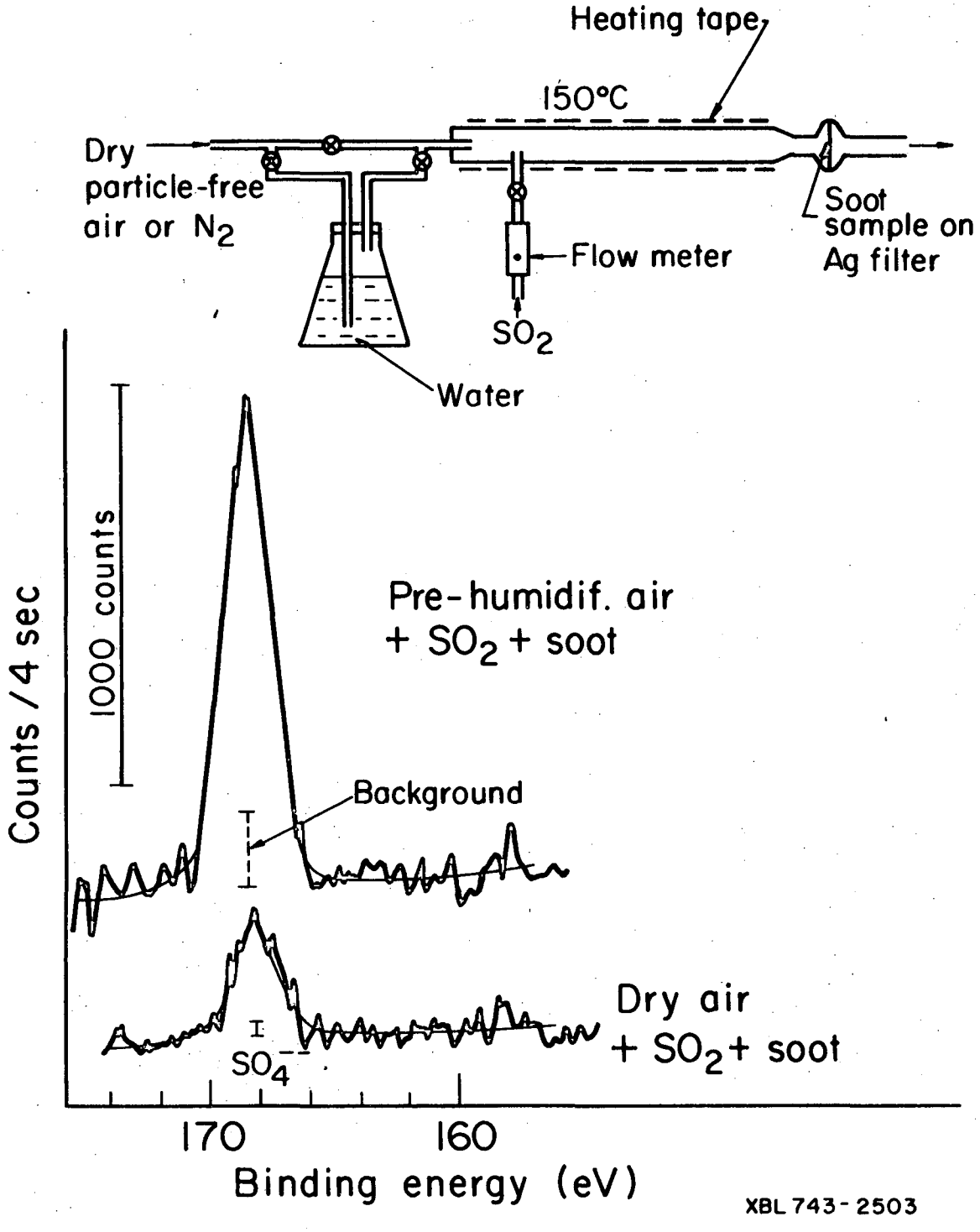
Heating tape
150°C
Dry
particle-free
air or N_2
Soot
sample on
Ag filter
Flow meter
SO_2
Water
1000 counts
Counts /4 sec
Pre-humidif. air
+ SO_2 + soot
Background
Dry air
+ SO_2 + soot
SO_4^{--}
170
160
Binding energy (eV)
XBL 743-2503

Figure 15

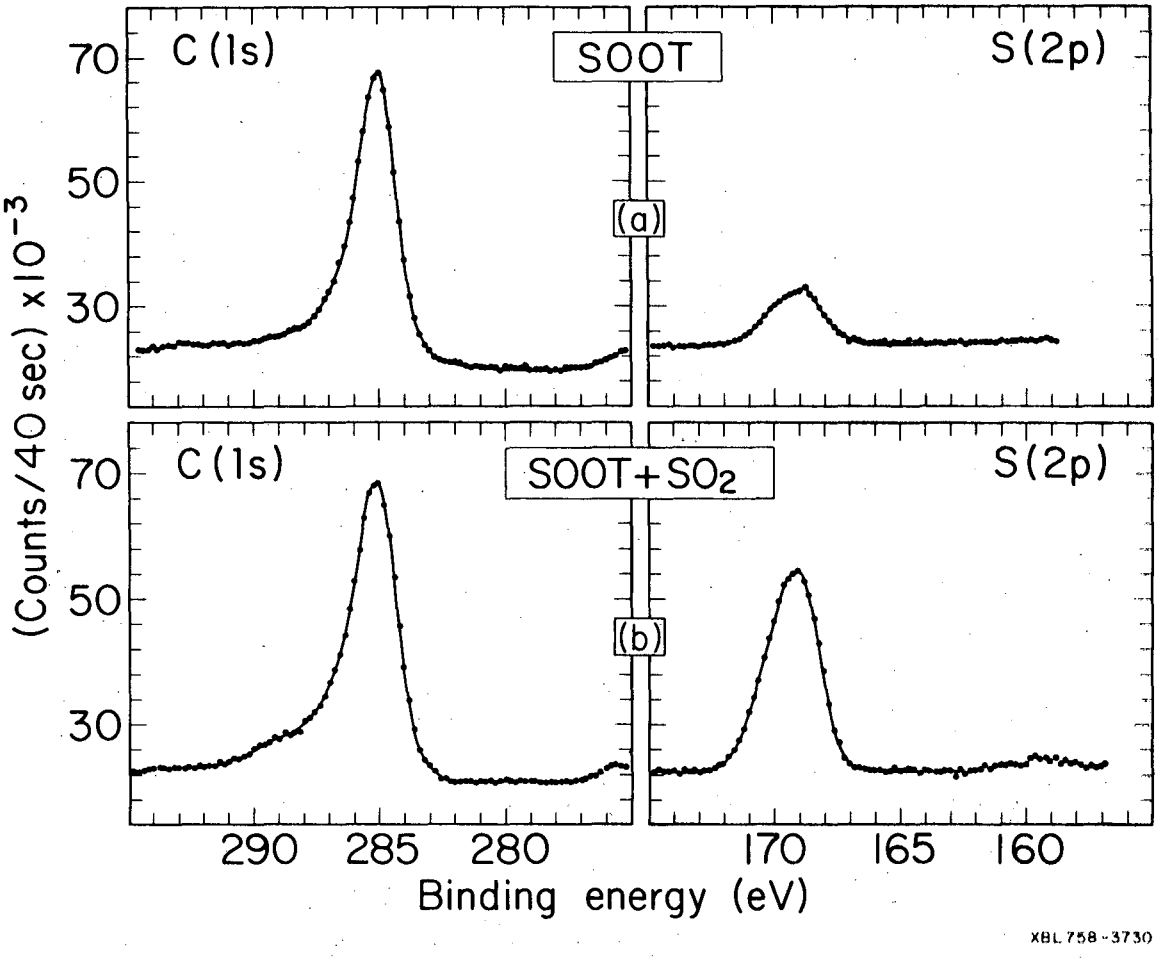

Figure 16

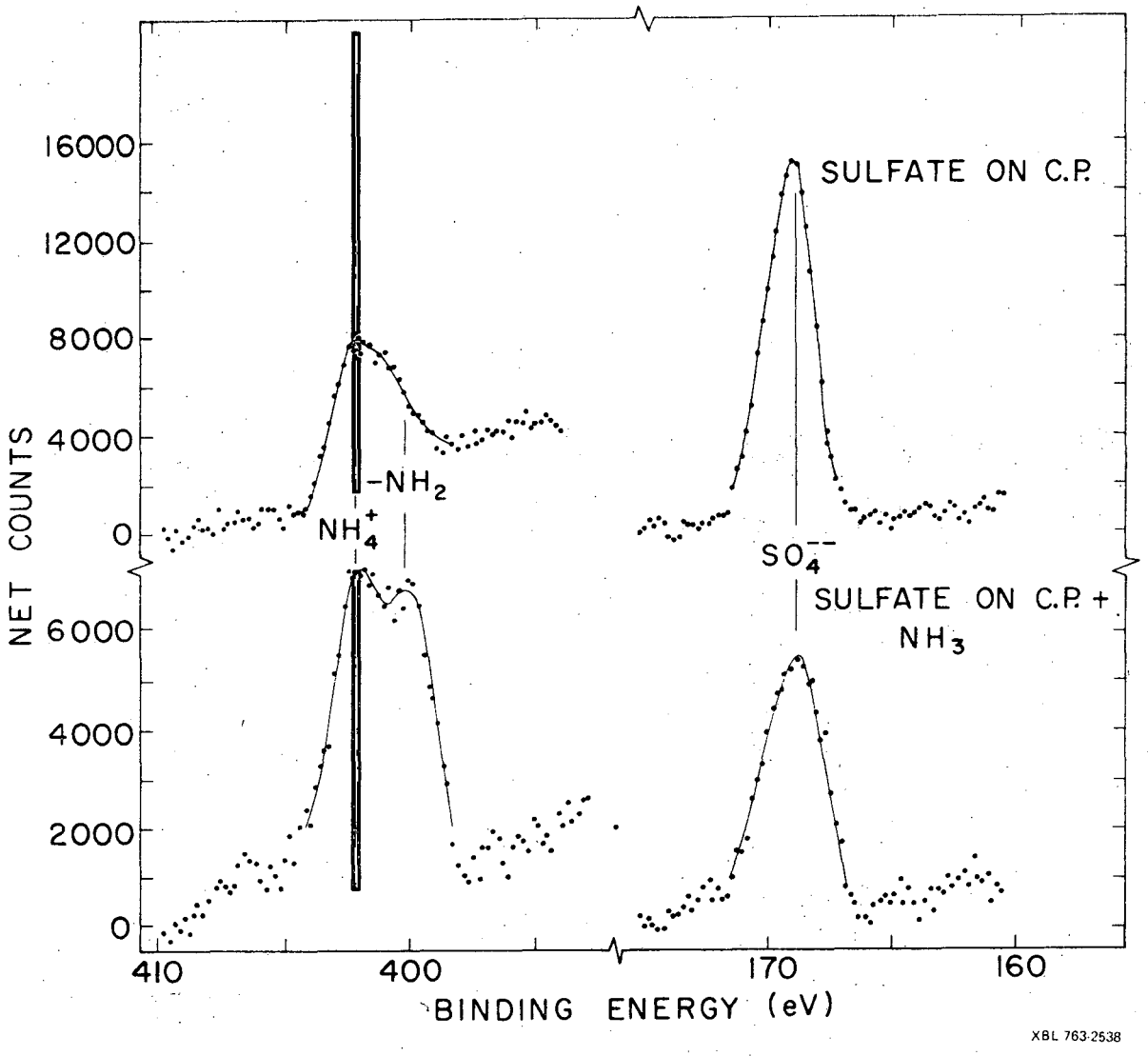
16000
12000
8000
4000
0
NET COUNTS
-NH2
NH4+
SULFATE ON C.P.
SO4--
6000
4000
2000
0
SULFATE ON C.P. +
NH3
410
400
170
160
BINDING ENERGY (eV)
XBL 763-2538

Figure 17

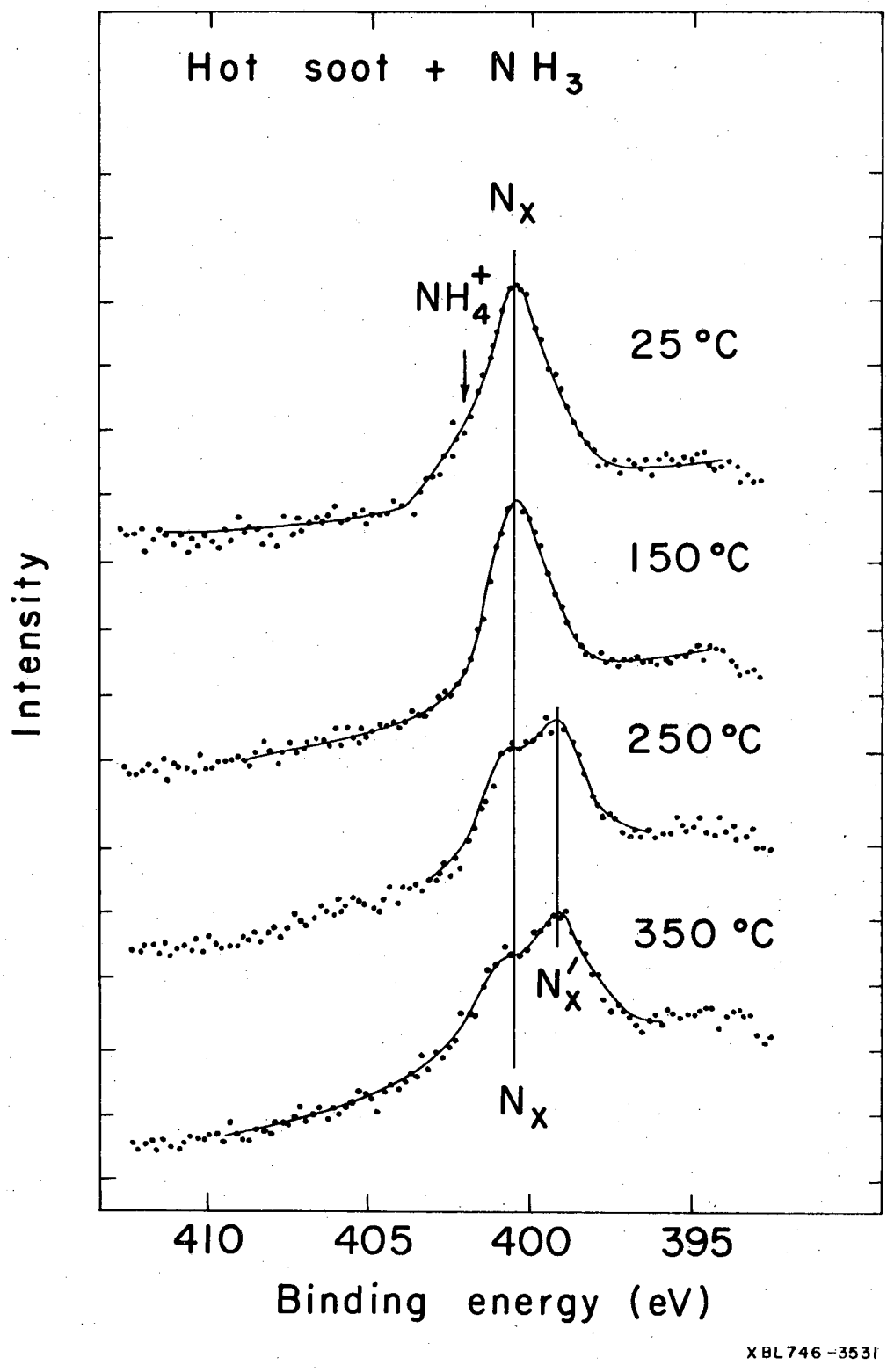

Figure 18

TECHNICAL INFORMATION DIVISION
LAWRENCE BERKELEY LABORATORY
UNIVERSITY OF CALIFORNIA
BERKELEY, CALIFORNIA 94720